



Assimilation of volcanic sulfur dioxide products from IASI and TROPOMI into the chemical transport model MOCAGE: case study of the 2021 La Soufrière Saint-Vincent eruption

Mickaël Bacles¹, Jonathan Améric¹, and Vincent Guidard¹

¹CNRM, Université de Toulouse, Météo France, CNRS, Toulouse, France

Correspondence: Mickaël Bacles (mickael.bacles@meteo.fr)

Abstract. Sulfur dioxide emitted during volcanic eruptions can be hazardous for aviation safety. As part of their activities, the Volcanic Ash Advisory Centres (VAACs) are therefore interested in the real-time atmospheric monitoring of this gas. A recent development aims at improving the forecasts of volcanic sulfur dioxide quantities made by the MOCAGE chemistry transport model. For this purpose, observations from both TROPOMI and IASI (B and C) instruments located on separate polar orbiting satellites are assimilated in the model. These sulfur dioxide measurements are based on the eruption event of the La Soufrière Saint-Vincent volcano in April 2021. Observations from the OMI instrument are considered as validation data. The resulting assimilation experiments show that the combined assimilation of IASI and TROPOMI observations always leads to a better forecast compared to the independent assimilation of data from each instrument. Sulfur dioxide atmospheric field forecasts are better when the available observations are numerous and cover a long time window.

10 1 Introduction

During volcanic eruptive events, large quantities of ash and sulfur dioxide (SO₂) are quickly released into the atmosphere. The emitted volcanic plumes can be transported far from the emission sources, reaching sometimes the upper troposphere or even the stratosphere (Carn et al., 2009). At such altitudes, volcanic ash plumes become hazardous for aviation safety as they can irreversibly damage aircraft engines and significantly lower flight visibility (Prata, 2009). Aircraft passengers and crew are also directly threatened, especially because air quality inside and at the vicinity of volcanic plumes is strongly degraded, generating respiratory issues detrimental to human health (Schmidt et al., 2014).

Some volcanoes are monitored by in situ sensors except if they are hardly reachable and hazardous. Consequently, passive satellite remote sensing remains an efficient technique providing global data on gases and aerosols emitted during volcanic eruptions. Sulfur dioxide is one of the compounds measurable by remote sensing. The absorbing bands of this gas are in the ultraviolet (UV \sim 310–340nm) and thermal infrared (IR - $\nu_1 \sim$ 8.6 μ m, $\nu_3 \sim$ 7.3 μ m and $\nu_1 + \nu_3 \sim$ 4 μ m) domains (Carn et al., 2016).

In many eruption cases like the one of the Icelandic volcano Eyjafjallajökull in 2010, volcanic sulfur dioxide can be considered as a tracer to predict volcanic ash dispersion (Sears et al., 2013). However, both ash and sulfur dioxide plumes need to be monitored separately as their spatial distribution do not always coincide perfectly (Thomas and Prata, 2011). A striking



25 example is the eruption case of the Icelandic volcano Grímsvötn in 2011, during which both sulfur dioxide and ash plumes were clearly separated (Prata et al., 2017).

Volcanic sulfur dioxide primary emissions can also be rapidly converted into secondary sulfate aerosols by reacting with water vapour and dioxygen. This conversion directly impacts the spatial distribution of volcanic sulfur dioxide plumes. The eruption of the Hunga Tonga volcano in January 2022 was exceptional as volcanic gases (sulfur dioxide and water vapour) and ash have been injected at least at 30km altitude (Witze, 2022). As a result, stratospheric sulfur dioxide has been rapidly converted into sulfate aerosols because of water vapour propelled in the stratosphere during the submarine eruption (Sellitto et al., 2022).

To guarantee aviation safety, pilots need to dispose of accurate data on volcanic plume extent, movement and chemical composition. The International Civil Aviation Organization (ICAO) and the World Meteorological Organization (WMO) created in 1987 the International Airways Volcano Watch (IAVW) for this purpose (Lechner et al., 2018). Since 1990, the IAVW system includes nine worldwide responsibility areas, each represented by a Volcanic Ash Advisory Centre (VAAC). Europe, Africa and Middle East are part of the Toulouse VAAC supervised by Météo-France (Gouhier et al., 2020).

Information on volcanic plumes provided by each VAAC to aviation authorities currently rely on specific services like the Support to Aviation Control Service (SACS) (Brenot et al., 2014) or the European Natural Airborne Disaster Information and Coordination System for Aviation (EUNADICS-AV) (Brenot et al., 2021). Based on in-situ measurements, satellite data and modelling products, these systems provide to the VAACs information on volcanic ash and sulfur dioxide plumes. The Toulouse VAAC forecasts the dispersion of volcanic ash plumes by running MOCAGE-Accident (Gouhier et al., 2020), a specific version of the three-dimensional chemistry transport model (CTM) MOCAGE (Modèle de Chimie Atmosphérique à Grande Échelle) of Météo-France. To achieve this, an injection profile and a quantity of ash emitted by the volcano, previously chosen by the forecaster, are used to predict the dispersion of the volcanic plume.

Assimilation of volcanic sulfur dioxide observations into a model has already been performed in several situations like for the eruption events of the Eyjafjallajökull in 2010 and the Grímsvötn in 2011. Volcanic sulfur dioxide released by these volcanoes has been monitored by the GOME-2 (Global Ozone Monitoring Experiment-2) and OMI (Ozone Monitoring Instrument) UV sensors. The resulting retrieved observations have been assimilated in the Integrated Forecasting System (IFS) of the European Centre for Medium-Range Weather Forecasts (ECMWF) by using the former Monitoring Atmospheric Composition and Climate (MACC) system dedicated to atmospheric composition. Initialising the model with sulfur dioxide analysis improved the sulfur dioxide plume forecasts (Flemming and Inness, 2013). Volcanic sulfur dioxide retrievals from GOME-2 and TROPOMI (Tropospheric Monitoring Instrument) UV sensors observations have been assimilated in the global CAMS (Copernicus Atmosphere Monitoring Service) assimilation system after the 2019 Raikoke volcanic eruption. On top of that, a retrieved volcanic sulfur dioxide layer height from the TROPOMI Layer Height product has been assimilated. Including plume height information into the assimilation system enhanced the quality of the forecasts made from the analyse fields (Inness et al., 2022).

In April 2021, the eruption of the La Soufrière Saint-Vincent volcano emitted a large amount of SO₂ into the atmosphere. This sulfur dioxide has been detected by several remote sensing instruments like the IR sensor IASI (Infrared Atmospheric



60 Sounding Interferometer), the UV sensors TROPOMI and OMI. The assimilation of TROPOMI, IASI and both instruments
should improve MOCAGE. Indeed, without data assimilation, the model does not simulate SO₂ plume. In this study, we
assimilate jointly an UV instrument, TROPOMI, and IR instruments, IASI B and IASI C allowing to correct the model during
both day and night. The use of instruments using different wavelengths to assimilate volcanic SO₂ data is also beginning to be
developed in IFS. In MOCAGE, a part of the SO₂ can be converted into sulfate aerosols, particles which are causing problems
65 in the aviation sector.

For the assimilation, the three-dimensional variational data assimilation system of the CTM MOCAGE (El Amraoui et al.,
2022) is used. Forecasts of volcanic sulfur dioxide plumes are then initialized by the resulting analyses. Two preliminary
experiments are conducted by assimilating independently total columns retrievals from IASI and TROPOMI sensors. The
resulting total columns of volcanic sulfur dioxide assimilated in MOCAGE are then compared to those measured by the OMI
70 independent sensor, located on another satellite.

In this paper, the La Soufrière Saint-Vincent eruption event of 2021 is introduced in the second part. Then, the assimilation
data provided by the corresponding instruments is described in the third part, before the chemical transport model MOCAGE
and its assimilation system in the fourth part. The fifth parts address the results of this case study.

2 Description of the 2021 La Soufrière Saint-Vincent eruption

75 La Soufrière Saint-Vincent is a volcano located in the Grenadines islands (13.33°N, 61.18°W). The eruption in 2021 started
on 9th April with a violent explosion around 12:40 UTC local time. This first explosion released a volcanic plume that reached
an altitude of 8 km. As a result, thousands of people were forced to flee. A second and weaker explosion occurred at 18:45
UTC, generating a volcanic plume that reached an altitude of 4 km. At 22:35 UTC, a third explosion took place with a plume
reaching 16 km. Between 10th April and 11th April in the morning, the volcanic activity became periodic as explosions occurred
80 every 1 to 3 hours, during short time periods of 20 to 30 minutes each. Although the number of explosions decreased from 12th
April, the volcanic plume remained at a high altitude, exceeding 12 km and sometimes even 16 km. Two last major explosions
took place on 12th April at 08:15 UTC and on 13th April at 10:30 UTC with plumes reaching altitudes of 12.8 km and 11 km
respectively. The volcano continued to emit temporarily ash and volcanic gases in the atmosphere until the 22nd April but the
plume from these explosions did not reach 8km high anymore. No fewer than 30 explosions were observed during this eruption
85 event, most of them during 9th April and 11th April. More information about the La Soufrière eruptions is available in the report
of Bennis and Venzke (2021).

3 Description of the instruments

3.1 TROPOMI

TROPOMI is a hyperspectral radiometer with spectral bands extending from the UV to the shortwave infrared (SWIR) domains.
90 This instrument is on board the polar orbiting Sentinel 5 Precursor (S5p) satellite whose goal is to provide information and

services on air quality and climate (European Space Agency, 2020). Since August 2019, TROPOMI benefits from a high spatial resolution of 5.5 km x 3.5 km at nadir. This instrument has a daily temporal resolution (no observation at night) and its overpass local time occurs at 13:35 UTC (Veeffkind et al., 2012).

Volcanic sulfur dioxide plumes can be globally monitored with the high spatial resolution of TROPOMI. Unprocessed
95 radiances measured by the instrument are often unpacked and formatted to become level 1 (L1) data. This data can then
be converted into a proper retrieved environmental variable as sulfur dioxide, forming a level 2 (L2) product. This conversion
requires the use of a retrieval algorithm having its own specificities and uncertainties. Historically, the first institutes elaborating
sulfur dioxide L2 products with TROPOMI measurements are the Royal Belgian Institute for Space Aeronomy (BIRA) and the
German Aerospace Center called DLR (Deutsches Zentrum für Luft- und Raumfahrt). For that, they use the differential optical
100 absorption spectroscopy (DOAS) algorithm, particularly fitted for TROPOMI operational near-real time processing (European
Space Agency, 2020).

Backscattered ultraviolet radiation is measured in order to construct absorption spectra. DOAS algorithm is then applied to
these spectra for different fitting windows between 310 nm and 390 nm. The DOAS algorithm operates in several steps. First,
slant column densities (SCD) are computed. They correspond to the integrated sulfur dioxide concentration along the mean
105 atmospheric optical path. Then, conversion factors called Air Mass Factors (AMF) are obtained from suitable radiative transfer
calculations to take measurement sensitivity changes into account. These changes depend on many factors like observation
geometry, total ozone absorption, clouds, surface reflectivity. Moreover, measurement sensitivity varies with the altitude of
the emitted sulfur dioxide plume. As this altitude is unknown, the AMF are computed for several hypothetical sulfur dioxide
vertical profiles. One profile used for polluted scenarios comes from a forecast made by the TM5 chemical transport model
110 (Huijnen et al., 2010). Three other profiles are available for 1 km thick boxes. The first box extends from the ground level
to 1 km high. The two others are centred at 7 and 15 km above mean sea level. The first profile is located in the boundary
layer and stands for well-mixed anthropogenic or volcanic sulfur dioxide conditions. The second profile aims at representing
sulfur dioxide emitted by effusive volcanic eruptions in the upper troposphere. The third one is for sulfur dioxide released
by explosive volcanic eruptions above the lower stratosphere (Theys et al., 2017). As four AMF are available depending on
115 different assumed SO₂ vertical profiles, the conversion of SCD into vertical column densities (VCD) generates four types of
VCD. These vertical columns correspond to the number of sulfur dioxide molecules in an atmospheric column per unit area,
usually expressed in Dobson Unit (1 DU = 2.69 · 10¹⁶ molecules.cm⁻²). Finally, averaging kernels are computed for the four
vertical profiles (Theys et al., 2019).

For our study, we use sulfur dioxide total vertical columns computed from the hypothetical profile centred around 15 km.
120 These columns are associated to their systematic errors in order to compute the observation error matrix of the MOCAGE
assimilation system. Moreover, the averaging kernel matrix needs to be considered for comparing TROPOMI to other instru-
mental measurements or model calculations (Rodgers and Connor, 2003). Finally, data is selected according to the category of
the TROPOMI detection. Many cases are taken into consideration in our study: flag 1 for sulfur dioxide detection, 2 for clear
volcanic detection and 3 for detection close to a known anthropogenic source. The quality of the SO₂ retrieval is given by a



125 quality flag with values ranging from 0 for uncertain retrieval to 1 for the best retrieval. TROPOMI data are available on the
NASA website (<https://disc.gsfc.nasa.gov/>, last access: 19th September 2024).

3.2 TROPOMI Layer Height product

The TROPOMI Layer Height product (Hedelt et al., 2019) allows to know the altitude of a SO₂ plume when TROPOMI SO₂
total columns are higher than 20 DU thanks to a machine learning algorithm called "Full-Physics Inverse Learning Machine"
130 (FP_ILM). Hedelt et al used the LInearized Discrete Ordinate Radiative Transfer model (LIDORT) (Spurr et al., 2008) to
simulate many reflectance spectra for different values of solar zenith angle (SZA), viewing zenith angle (VZA), relative az-
imuth angle (RAA), O₃ and SO₂ vertical column density, layer height, surface albedo and surface pressure. Before classifying
these reflectance spectra in ten principal components (PC), TROPOMI instrument spectral response function, characterising
the sensitivity of the instrument across its measurement spectrum, is applied. These PCs and information about the surface,
135 O₃ total columns, SZA, VZA and RAA are used as an input of the neural network. SO₂ total columns and SO₂ height are
diagnosed thanks to the neural network. In this study, SO₂ total columns diagnosed by the neural network are not assimilated.
Nevertheless, SO₂ height product is used to validate the altitude of the modelled plume.

TROPOMI Layer Height data are available on the NASA website (<https://disc.gsfc.nasa.gov/> from 17th July 2023; last
access: 12th April 2024. Older data were provided by the German Aerospace Center (DLR),

140 3.3 IASI

IASI is a Fourier transform spectrometer operating in the IR spectral domain. This instrument is located on both polar orbiting
MetOp-B (IASI B) and MetOp-C (IASI C) satellites. The best spatial resolution at nadir is a circle which diameter is 12 km.
Twice a day (measurements are possible both at daytime and nighttime), IASI are observing around 09:30 local time and
around 21:30 local time (Clerbaux et al., 2009).

145 Sulfur dioxide observation data provided by IASI measurements are converted into a level 2 product by using the ULB-
LATMOS retrieval algorithm (Clarisse et al., 2012). In our study, we use an optimal sulfur dioxide total vertical column
computed from an estimated altitude of the volcanic plume. This estimation is based on another algorithm created for IASI
sulfur dioxide plume altitude retrievals (Clarisse et al., 2014). IASI data are available at the AERIS data centre (<https://iasi.aeris-data.fr/>, last access: 19th September 2024).

150 3.4 OMI

OMI is a multispectral radiometer with spectral bands extending from the UV to the visible (VIS) domains. This sensor is
carried by the polar orbiting Earth Observing System (EOS) Aura satellite. The best nadir spatial resolution is about 24 km x
13 km. Since 2011, this instrument has a two-day daily coverage with an overpassing at 13:45 local time (Qu et al., 2019).

155 OMI sulfur dioxide total vertical columns are used as independent observations to check the results of our assimilation ex-
periments. These total vertical columns are retrieved thanks to an algorithm based on a principal component analysis (PCA)



technique (Li et al., 2017). These vertical columns are computed by considering a hypothetical sulfur dioxide plume altitude located around 18 km. OMI data are available on the Earthdata Nasa website (<https://omisips1.omisips.eosdis.nasa.gov/outgoing/OMSO2NRTb/>, last access: 19th September 2024).

4 Description of the SO₂ assimilation experiments

160 MOCAGE (Modèle de Chimie Atmosphérique à Grande Echelle) is the CTM developed by the Centre National de Recherches
Météorologiques (CNRM) at Météo-France (Josse et al., 2004). It has many operational uses such as air quality forecasting
over France (Rouil et al., 2009) and over Europe with the contribution to the CAMS ensemble forecasting system (Marécal
et al., 2015). MOCAGE is also used in an accident mode by the Volcanic Ash Advisory Centre of Toulouse (VAAC) when a
volcanic eruption or an industrial accident occurs.

165 4.1 The model and its assimilation system

The CTM MOCAGE is a model using a semi Lagrangian scheme for the transport of chemical species which can be global or
nested. It enables to predict chemical evolution of the atmosphere up to 4 days. In this study, we use MOCAGE on a 1 ° global
domain with 47 hybrid σ pressure levels distributed between the surface and 5 hPa (7 in the planetary boundary layer, 20 in the
free troposphere and 20 in the stratosphere).

170 MOCAGE is an offline model and needs meteorological fields like wind speed and direction, temperature, humidity, pressure,
rain, and clouds from a Numerical Weather Prediction (NWP) model or from a climate model. In this study, meteorological
forcings are provided by the French NWP model Action de Recherche Petite Echelle Grande Echelle (ARPEGE) (Courtier,
1991; Bouyssel et al., 2022).

175 The model enables to transform species according to the chemical scheme RACMOBUS which is a combination of two
chemical schemes. The first one, RACM, is computed for the tropospheric chemical reactions (Stockwell et al., 1997). It is
completed with the sulfur cycle (Feinberg et al., 2019). The second chemical scheme, REPROBUS, is used for the stratospheric
chemical reactions (Lefevre et al., 1994). Every 15 minutes, MOCAGE model provides the atmospheric composition of 112
gaseous species thanks to 379 chemical reactions and 57 photolysis reactions.

180 Both primary and secondary aerosols are modelled in MOCAGE (Guth et al., 2016), (Sič et al., 2015). Primary aerosols
include desert dust, sea salt, black carbon, organic carbon and volcanic ash. In this study, volcanic ash modelling is turned
off. Secondary inorganic aerosols are represented by sulfate, nitrate and ammonium aerosols. The aerosol size distribution is
described by a sectional approach, with six size sections delimited by the following diameters: 0.002–0.01; 0.01–0.1; 0.1–1.1;
1.1–2.5; 2.5–10 and 10–50 μm . Desert dust and sea salt emissions depend on the wind strength and the type of the ground.

185

To forecast air quality, emissions of gaseous and aerosol species need to be taken into account by the model. Emission
inventories are therefore used, such as the MACCity inventory for anthropogenic emissions (Lamarque et al., 2010) and the



MEGAN inventory for biogenic emissions (Sindelarova et al., 2014). Sulfur dioxide released into the atmosphere by passive degassing can be, as in our study, also part of the emissions included in the model (Lamotte et al., 2021). Daily emissions of biomass burning provided by the Global Fire Assimilation System (GFAS) (Kaiser et al., 2012) are injected into the model at many vertical levels, depending on the latitude of fires (Cussac et al., 2020). Other species except lightning nitrogen oxides (Nox) (Price et al., 1997) and aircraft emissions (Lamarque et al., 2010) are emitted on the first five levels of the model (approximately 500m altitude).

Many species can be assimilated in MOCAGE. This is the case for gaseous species, such as O₃ (Emili et al., 2014), (El Aabaribaoune et al., 2021), (Vittorioso et al., 2024). Aerosols are also assimilated in MOCAGE (Descheemaeker et al., 2019), (Sič et al., 2016), (El Amraoui et al., 2022), (Cornut et al., 2023).

The assimilation system used in this study is the 3D-VAR, described hereafter. A short-range forecast from MOCAGE x^b and observations y are combined to find the optimal state x^a , taking into account their respective error covariance matrices B and R. x^a can be searched as the sum of $x^b + \delta x^a$ where δx^a is the increment minimising the cost function J:

$$J(\delta x) = \frac{1}{2}(\delta x)^T B^{-1}(\delta x) + \frac{1}{2}(y - \mathcal{H}[x^b] - \mathcal{H}[\delta x])^T R^{-1}(y - \mathcal{H}[x^b] - \mathcal{H}[\delta x]) \quad (1)$$

\mathcal{H} is the observation operator used to obtain the model data in the observation space. Before running an assimilation experiment, a full description of R and B matrices is required. The background error covariance is spread on many vertical levels and on many meshgrid thanks to the correlation matrix. In MOCAGE, the vertical and horizontal correlations are described as gaussian functions.

4.2 TROPOMI and IASI data assimilation setup

Several hourly 3D-VAR assimilations of volcanic SO₂ data have been conducted over the specific eruptive period from 9th April to 15th April 2021 into MOCAGE with a 1° horizontal resolution. Different simulations have been carried out, one with the assimilation of IASI B and C (iasi_assim), one with the assimilation of TROPOMI (tropomi_assim), another with the assimilation of IASI and TROPOMI and the last one without assimilation (Table 1). The results of these experiments are compared to OMI observations.

In these experiments, IASI and OMI observations above 0.5 DU are used. This value corresponds to the lowest total columns measurable by these instruments (Koukouli et al., 2022), (Qu et al., 2019). For TROPOMI instrument, observation retrievals with a SO₂ peak concentration at 15km of high are used. Moreover, an observation is used when the quality flag is above 0.5 and if the slant column is above 1 DU, matching the noise of the instrument.

Averaging kernels are taken into account in this study. For TROPOMI, averaging kernels are only given for the a priori profiles from the TM5 CTM. Nevertheless, averaging kernels for the other a priori profiles can be estimated by multiplying them by a scaling factor (Theys, 2018) as described by the following equation:



| Experiment | Assimilation of TROPOMI | Assimilation of IASI B and C | Assimilation of OMI |
|---------------|-------------------------|------------------------------|---------------------|
| iasi_assim | No | Yes | No |
| tropomi_assim | Yes | No | No |
| joint_assim | Yes | Yes | No |
| dry | No | No | No |

Table 1. Description of the performed experiments during this study with the different assimilated instruments.

$$220 \quad AVK(z) = \frac{AVK_{TM5}(z) \times AMF_{TM5}(z)}{AMF_{15km}} \quad (2)$$

with $AVK(z)$ the averaging kernels at a given altitude, $AVK_{TM5}(z)$ and $AMF_{TM5}(z)$ the averaging kernels and the air mass factor at the altitude z from the TM5 CTM and AMF_{15km} the air mass factor for the a priori profile containing a peak at 15km of altitude.

For IASI, averaging kernels are not given in the observation files. However, they can be computed at many heights thanks to
 225 the SO_2 total columns, according to the following equation:

$$Avk(z) = \frac{Y(z)}{Y(z_{ref})} \quad (3)$$

with z the hypothetical SO_2 injection altitude, $Avk(z)$ the averaging kernels at a given altitude z , $Y(z)$ the total columns computed for a SO_2 injection at the altitude z and $Y(z_{ref})$ the total column computed for a reference altitude injection. In our case, this altitude is provided by the observation files.

230 In this study, we assume there is no spatial correlation in the observation error. For TROPOMI, observation error covariance is directly computed from satellite data. The uncertainties of IASI measurements vary according to the value of the total column measured. In the case of this eruption, IASI measured total SO_2 columns ranging from 0.5 to 20 DU. The uncertainties in this range of observations vary from around 25% to 5% of the observation (Clarisse et al., 2012). For IASI, we set the observation error standard deviation to 15% of the observation values. Correlation matrix is the same in all experiments with
 235 data assimilation.

For observations stronger than 20 DU, TROPOMI Layer Height product is able to diagnosed the altitude of the plume. During this volcanic eruption, 90% of the diagnosed heights are between 9 and 21 km. Consequently, to force SO_2 injection between these two altitudes, we chose a profile containing strong values (1e-8 ppv) between altitudes of 9 and 21 km as back-
 240 ground error standard deviation.

As in the operational mode of MOCAGE, a forecast initialised by the assimilation outputs is launched at 00 UTC each day. In our study, this forecast is performed up to a 72 h term range.



5 Impact on analyses

245 5.1 Impact on SO₂ and sulfate

The assimilation of SO₂ total column measurements significantly enhances MOCAGE's ability to describe SO₂ plumes. When no observations are assimilated, no SO₂ plume is represented by the model. However, when satellite observations are assimilated, a SO₂ plume is simulated and corrected more or less frequently depending on the instrument or combination of instruments and thus on the overpass time of the corresponding satellites.

250

Figure 1 shows the SO₂ total columns observed and analysed on 10th April 2021 at various times (02, 14, 16 and 17 UTC). The observations are depicted on the first line for TROPOMI, the second and the third lines for IASI B and C respectively. The model's outputs are shown on the fourth line for the `iasi_assim` experiment, on the fifth line for the `tropomi_assim` experiment and on the sixth line for the `joint_assim` experiment. At 02 UTC, the `tropomi_assim` simulation does not present a
255 SO₂ plume, in contrast to the plume modelled with IASI assimilation. Nevertheless, the model underestimates the total column values against the IASI observations. Due to the use of UV wavelengths, TROPOMI is unable to measure SO₂ total column during night. Consequently, no SO₂ plume is modeled in MOCAGE until 17 UTC. Before the overpass of TROPOMI, IASI instruments measure SO₂ total columns once again. It allows to increase both intensity and size of the plume in MOCAGE at 14 UTC. At 17 UTC, a plume appears in the `tropomi_assim` experiment thanks to the TROPOMI overpass. Compared to
260 the TROPOMI observations, high total columns values are underestimated by MOCAGE. At this time, the simulated volcanic plume in the `iasi_assim` experiment is slightly smaller and weaker than the plume in the `tropomi_assim` experiment and the TROPOMI observations. Assimilation of TROPOMI data allows to simulate a strong area value in vicinity of the volcano in both `tropomi_assim` and `joint_assim` experiments. This structure of strong values is not modeled with the IASI data assimilation because it corresponds to the latest volcanic SO₂ emission. This new release, due to a new eruption event, took place between
265 the IASI and the TROPOMI overpasses. Simulated SO₂ total columns in `joint_assim` experiment are stronger, in particular around 55°W where observations are strong. For this part of the plume, the difference between the model and the observations is weaker because it is analysed five times during this day whereas the model is corrected four times when IASI is assimilated and only once when TROPOMI is assimilated. The greater the number of model corrections, the smaller the differences between observations and the model. In this experiment, the shape of the plume is slightly different with a pattern around 39°W
270 which is simulated with the IASI data assimilation and not with the TROPOMI one.

Figure 2 shows the SO₂ total columns observed and analysed on 11th April 2021 at 11, 13, 17 and 18 UTC. Until 17 UTC not included, the SO₂ plumes simulated by the `iasi_assim` and the `joint_assim` experiments are similar. At 11 UTC, the eastern parts of the plume are consistent between experiments. Thanks to the IASI overpass at the end of the previous day, the plume is closer to the volcano and SO₂ total columns of the western part of the plume are stronger compared to the `tropomi_assim`
275 experiment. At 13 UTC, IASI SO₂ total columns are assimilated, reducing the SO₂ plume over the ocean and increasing the values in the vicinity of the volcano into the model. At 17 UTC, TROPOMI observations are assimilated and the shape of the SO₂ plume is consistent between the experiments. The SO₂ plume is more extended with the assimilation of TROPOMI.



Concerning the values of the total columns, strong values areas are more intense with the assimilation of both instruments, particularly near the volcano and in the middle of the Atlantic Ocean. At 18 UTC, the OMI overpass enables to validate these
280 experiments with independent observations. The SO₂ plume simulated by the joint_assim experiments seems to be the closest to OMI observations. Indeed, in this experiment, the strong SO₂ total columns patterns match better to the observations, in particular around 39°W and around 55°W.

The vertical cross-section at 13.5°N, illustrated in figure 3, presents the vertical SO₂ concentrations at various times on 11th April 2021 (11, 13, 17 and 18 UTC). The chosen assimilation settings result in a plume that extends from 9 to 21 km in
285 altitude. Until 17 UTC not included, the altitude of the maximum SO₂ concentration in the different experiments is consistent with an altitude around 13 km to 17 km. The lowest concentrations are simulated in the tropomi_assim assimilation. At 11 UTC, the IASI assimilation of the end of the previous day enables to simulate a plume located closer to the volcano compared to the tropomi_assim experiment. At 13 UTC, with the assimilation of IASI, a new strong concentration pattern appears near the volcano around 13 km of altitude. At 17 UTC, in experiments where TROPOMI observations are assimilated, SO₂
290 concentration increases around 9km of altitude in vicinity of the volcano The altitude of the plume is closer to the TROPOMI Layer height product in the joint_assim experiment. However, around 50°W, TROPOMI Layer Height product shows a plume between 10 km and 16 km of altitude. In the experiments, the height of the plume varies between 15 km and 20 km, which is too high compared to the TROPOMI Layer Height Product. Nevertheless, around 50°W, few observations meet the criteria for TROPOMI_LH to be able to diagnose the height of the plume. It is difficult to conclude whether the plume altitude is correctly
295 represented in the model when there are few or no observation above 20 DU.

SO₂ can be converted into sulfate aerosol in the presence of water vapour. This process is modelled in MOCAGE. Indeed, sulfate total columns show structures in the assimilation experiment which are not shown without assimilation.

Figure 4 shows the SO₂ total columns on top panel, the sulfate total columns on the middle panel and the Aerosol Optical Depth (AOD) on the bottom panel on 14th April 2021 at 07 UTC for different experiments with assimilation (iasi_assim,
300 tropomi_assim and joint_assim) and without assimilation (dry). This figure shows strong differences between each experiment. Indeed, at this date, the analysed SO₂ total columns are stronger by assimilating TROPOMI instrument than in the iasi_assim and the joint_assim experiments. Nevertheless, SO₂ total column values never reach 3 DU. Without assimilation, no SO₂ plume is modelled by MOCAGE.

The assimilation of volcanic SO₂ total columns allows the model to simulate sulfate aerosols (figure 4 on the middle panel).
305 Indeed, a sulfate plume is simulated from the volcano to Guinea. This sulfate plume is not modelled in the experiment without assimilation. In the tropomi_assim experiment, strong sulfate total columns are simulated in French Guiana and in Venezuela. In this area, values exceed 25 mg/m² whereas values do not reach 20 mg/m² in iasi_assim and joint_assim experiments. Elsewhere the modelled sulfate total columns are consistent with from one assimilation experiment to another.

310 Total AOD are slightly increased in Central America with the SO₂ assimilation (figure 4 on fifth line). This rise is more important by assimilating TROPOMI in French Guiana and in Venezuela where AOD reach 0.5 against 0.4 in the iasi_assim and in the joint_assim experiments and 0.3 without assimilation (figure 4 on fourth line). However, few AOD observations



from MODIS (Moderate-Resolution Imaging Spectroradiometer) and VIIRS (Visible Infrared Imaging Radiometer Suite) instruments are available in this area. This makes it impossible to validate AOD assimilation.

315 **5.2 Impact of the assimilation on the detection of SO₂ threshold exceedances**

To assess the impact of assimilation on volcanic SO₂, the number of grid cells reaching 1 DU and 5 DU thresholds, over a sub-domain extending from 90°W to 40°E and from 20°S to 30°N, has been calculated and plotted on the figure 5 for the simulations: iasi_assim in red, tropomi_assim in blue and joint_assim in green, and for the observations: TROPOMI in orange, IASI B in purple, IASI C in magenta and OMI in grey. Since there are often several observations per grid cell, we looked at
320 the number of grid cells where the minimum and maximum of the total columns exceed these thresholds. These values are represented by horizontal lines. The number of grid cells where the median of the observations is superior to these thresholds is shown by a dot. Finally, the limits of the bars represent the number of grid cells where the 25th and 75th quantiles exceed the thresholds.

Between the 9th April and the 11th April 2021, the number of meshes where the median of observations exceeded 1 DU is
325 consistent between instruments. After this date, there were more grid cells where the median number of observations exceeded 1 DU with TROPOMI. Moreover, with this instrument, the dispersion of observations is high. There are few grid cells where all the observations exceed 1 DU, whereas on 14th April, there were more than 1200 grid cells where the maximum number of observations reach 1 DU. This dispersion is lower for instruments with lower resolutions. For IASI, the number of grid cells where the median of observations is superior or equal to 1 DU varies less than with UV instruments. This can be explained by
330 IASI's high sensitivity to water vapour, which masks part of the SO₂ column.

In the assimilation experiments, the number of points where the total column reach 1 DU is identical between iasi_assim and joint_assim until the end of the day on 10th April 2021. Until this date, the number of grid cells where the total column reaches 1 DU is zero with the TROPOMI assimilation. After this date, the number of grid cells where the total column exceeds 1 DU is always bigger in the joint_assim experiment. The number of grid cells above 1 DU is lower when only TROPOMI
335 is assimilated in the morning until 11th April. This number is smaller when only IASI is assimilated. The differences in the number of grid cells exceeding 1 DU are greater at the end of the study period. Until 11th April 2021 in the experiments where TROPOMI was assimilated and until 12th with the assimilation of IASI alone, the number of grid cells where the model exceeded 1 DU was consistent with the number of grid cells where the median of the observations exceeded this threshold. After this date, the number of grid cells exceeding 1 DU exceeds the number of meshes where the 75th quantile of TROPOMI
340 observations exceeds 1 DU. Whatever the instruments used, the number of points above 1 DU is too high compared to IASI and OMI observations. This shows that the extension of the SO₂ plume is too large in the model.

The number of grid cells with observations exceeding 5 DU is lower and similar for each instrument. On 9th, on 14th and on 15th April 2021, none of the observations exceeded this threshold. In the model, no column exceeds 5 DU for these dates.
345 Generally, the number of SO₂ columns exceeding 5 DU in the model is similar to the number of grid cells where the median of observations exceeds 5 DU. Between the end of the day on 10th and 12th April, the number of meshes is slightly greater by



assimilating the 2 instruments and is closer to the number of meshes where the median of the OMI observations reaches 5 DU even if the number of points above 5 DU is slightly underestimated at the end of the day on 10th April 2021. On this day, this number is underestimated in the model because a new eruption took place between the last assimilation of TROPOMI and the
350 overpass of OMI. On 11th April, the TROPOMI assimilation added a significant number of points above 5 DU in the model because of a large number of TROPOMI observations above 5DU. On 12th April, the extension of the plume reaching 5 DU is greater when assimilated in the tropomi_assim experiment. In fact, the value of the total columns falls in the model thanks to the assimilation of IASI. The TROPOMI overpass at the end of the afternoon also reduces the modelled total columns. The number of points above 5 DU in the model becomes similar.

355

To assess the accuracy of the model in simulating SO₂ total columns, a threshold-based analysis was implemented. The goal was to determine the number of instances where both the observations and the model successfully identified SO₂ total columns above certain thresholds (labelled as Hits), as well as the instances where the observations exceeded these thresholds but the model failed to detect them (labelled as Misses). Using these metrics, we defined the Probability of Detection (POD),
360 a ratio that ranges from 0 to 1. The POD is calculated by dividing the number of Hits by the sum of Hits and Misses for a given threshold. A POD score of 1 indicates a perfect detection by the model, meaning that all observed instances above the threshold were correctly simulated. On the other hand, a POD of 0 signifies that none of the observed SO₂ total columns above the threshold were detected by the model. The POD is computed with the following equation:

$$POD = \frac{Hits}{Hits + Misses} \quad (4)$$

365 Figure 6 shows the Probability of Detection (POD) computed for 1 DU and 5 DU thresholds against TROPOMI, IASI and OMI observations. Dots represent times when there is no observation. Crosses represent the moments when simulated SO₂ total columns are under a threshold whereas some observations exceeds this threshold. Against TROPOMI instrument, POD values are generally better in the experiments in which TROPOMI observations have been assimilated. In these experiments, POD values exceed 0.75 until the 13th April. The POD values are over 0.75 until 11th April in iasi_assim experiment. POD
370 values decrease at the end of the study period. For the 5DU threshold, POD values are slightly higher in joint_assim experiment, especially on 10th and 11th April, when around 100 TROPOMI observations exceed 5 DU. On 12th April, POD values are around 0.25 in the experiments in which TROPOMI instrument is assimilated. The model did not SO₂ total columns higher than 5 DU for this date in iasi_assim experiment. Between the 13th and the 15th April and on 9th April, no SO₂ total column above 5 DU is simulated in MOCAGE. For these days, between 1 and 9 observations above 5DU are measured by TROPOMI.

375

POD values, computed for a 1 DU threshold and with IASI observations, exceed 0.9 until 12th April in experiments in which IASI instruments are assimilated. No SO₂ total column is simulated with the TROPOMI assimilation until 10th April because TROPOMI overpasses the plume after IASI. In the morning of 9th April, no observation above 1 DU is detected by IASI. From 11th April, POD values are not null in the tropomi_assim experiment but they are smaller than the one calculated



380 from the `iasi_assim` and `joint_assim` experiments. In the afternoon of 9th April, only one observation above 5 DU is measured by IASI. At this location, the total column is under 5 DU. For these threshold and compared to `tropomi_assim` experiment, the probability to simulate high SO₂ total columns increases thanks to the IASI assimilation. Despite numerous observations above 5 DU, many events are missed on 10th April with a POD reaching nearly 0.4 in the morning and 0.5 in the afternoon. Most of simulated SO₂ total columns are between 1 DU and 5 DU. The maximum of POD is obtained on 11th April after the
385 assimilation of many observations measured by IASI exceeding 5 DU on 10th and on 11th April.

When comparing with OMI observations, the POD values computed with a 1 DU threshold are often consistent between the `tropomi_assim` and the `joint_assim` experiments. POD values are slightly better in `joint_experiment` on 11th and 12th April. One exception occurs on 9th April when POD value is higher by assimilating IASI instruments. For the 5 DU threshold, POD value is greater with the `joint_assim` experiment on 10th and 11th April. On 12th and 13th April, no SO₂ total column above 5
390 DU is modelled by MOCAGE whereas OMI measured observations above this threshold. Elsewhere in the study period, no observation greater than 5 DU is measured by OMI instrument and modelled by MOCAGE.

In the various modelling experiments, assimilating SO₂ total column data enhances the performances of the CTM MOCAGE by enabling the simulation of a SO₂ plume. However, for the lowest concentration threshold, the simulated SO₂ plume tends to be overly extensive, and the corresponding SO₂ burden is too high when compared to observational data. Nevertheless, for
395 higher thresholds, SO₂ plume area and SO₂ burden are consistent with the observations in the experiments where TROPOMI instrument is assimilated. Especially for the strong thresholds, POD values show an improvement of the model when both IASI and TROPOMI instruments are assimilated.

6 Impact of assimilation on forecasts

In this part, we study the impact of the assimilation on forecasts. To initialise the forecast, we use the assimilation outputs from
400 the `joint_assim` experiment. We use the term D0 for a 24h range term forecast, D1 for a 48h range term forecast and D2 for a 72h range term forecast.

On the figure 7, the fourth and the fifth line show SO₂ total column forecast for the 12th April 2021 at 01, 13, 15, 16 and 17 UTC. These lines represent respectively a forecast initialised by the 11th April 2021 analysis outputs and by the 10th April 2021 analysis outputs. SO₂ total column observations are plotted on the first line for TROPOMI, the second and the third line
405 for IASI and on the last line for OMI. When the model forecasts are initialised by the 9th April analysis outputs, no SO₂ total column value greater than 1 DU is present because even if the eruption started on 9th April, none of the assimilated instruments overpass the plume on this day. Using the results of the analysis on 10th April enables to the model to simulate a SO₂ plume which reaches West Africa. The observations show a plume reaching Africa but also the vicinity of the volcano. The western part of the plume is not modelled by MOCAGE on 12th April 2021 with the use of 10th April analysis outputs because the last
410 assimilation took place almost 2 days before. The more recent SO₂ emissions can not be simulated. Nevertheless, the part of the already simulated plume matches well with the observed plume intensity. Using the latest available analysis outputs from 11th April, MOCAGE predicts a plume which shape is closer to the observed one but it is always smaller. However, the model



tends to overestimate the total intensity of the SO₂ column compared to the TROPOMI and IASI measurements. In addition, using the latest available analysis predicts a SO₂ plume closer to the volcano.

415 Figure 8 represents the number of grid cells exceeding 1 DU and 5 DU for the D0 forecast in blue, for the D1 forecast in red and for the D2 forecast in green. Number of grid cells exceeding these thresholds are computed for TROPOMI in orange, IASI B in purple, IASI C in magenta and OMI in grey. We looked at the number of grid cells where the minimum and maximum of the total columns exceed these thresholds. These values are represented by horizontal lines in the figure 8. The number of grid cells where the median of the observations exceeds these thresholds is shown as a dot. Finally, the limits of the bars represent
420 the number of grid cells where the 25 and 75 quantiles exceed the thresholds.

Generally speaking, the number of meshes exceeding 1 DU or 5 DU decreases with the forecast period. This was not observed on 9th and 10th April, when no mesh exceeded 1 DU. The D0, D1 and D2 forecasts show the presence of a plume from 11th, 12th and 13th April 2021. These forecasts are initialised by the output of the assimilation of 9th April, i.e. before
425 the beginning of the eruption. On 11th April, there were around 200 grid cells where the model exceeded 1 DU for the D0 forecast. This number corresponds to the minimum number of grid cells where the TROPOMI and OMI observations reach 1 DU and is below the number of grid cells where the median of the IASI observations reaches 1 DU. On 12th April, the plume forecast with D0 was larger, with around 500 meshes exceeding 1 DU, corresponding to the number of meshes where the 25th quantile of the TROPOMI observations reached 1 DU and also where the median of the OMI observations reached
430 this threshold. After this date, the number of occurrences of the total column in SO₂ exceeding 1 DU increases and becomes greater than the number of grid cells where the IASI and OMI observations reach 1 DU. However, this number remains smaller than the maximum number of meshes calculated using TROPOMI observations. The number of points where the total column reaches 1 DU decreases with the forecast term range. Nevertheless, this number always exceeds the number of grid cells where the OMI and IASI observations reach 1 DU from 14 April onwards. Regarding the 5 DU threshold, no grid cell exceeds this
435 threshold for the D2 forecast. The D1 forecast shows a low number on 12th April when the total columns reach 5 DU. However, this number is similar to the number of grid cells where the median of TROPOMI and IASI observations reaches 5 DU. In addition, for this day, the number of points where the model reaches 5 DU is similar between the D0 and D1 forecasts. For 11th April, the number of occurrences of a total column greater than or equal to 5 DU is low in the model compared with the UV instruments. This number is within the range of grid cells where IASI observations exceed 5 DU.

440 The figure 9 represents the POD metric calculated by comparing the observations and the forecasts at several time steps for 1 DU and 5 DU thresholds. Whatever the thresholds used, in the D0 forecast, plume is well represented with the strongest POD values even if the POD values decrease compared to the obtained values computed with the analysis outputs. It indicates a rise of the number of Misses events. For the lowest threshold and for a D0 forecast, POD values reach at maximum 0.6 on 12th April 2021 and 13th April 2021 compared to TROPOMI, nearly 0.75 on 12th April 2021 compared to IASI and 0.7 on 13th
445 April compared to OMI. These values become lower with the increase of the forecast range except on 15th April and 16th April with TROPOMI. For larger threshold, Misses events dominate the 24 h and the 48 h forecasts. Moreover, POD values decrease in the D0 forecast when the threshold value increases. The forecasts initialised by the assimilation outputs are improved, in

particular when the most recent analysis is used to forecast and for lower SO₂ total columns. Nevertheless, for higher SO₂ total columns, MOCAGE encounters difficulties in accurately modelling such intense SO₂ total columns.

450 Incorporating SO₂ total column analysis outputs in the MOCAGE forecasts enhances its ability to model SO₂ plume. In the absence of the assimilation, the model fails to forecast the presence of a SO₂ plume. The use of recent analysis outputs progressively aligns the predicted location of the plume with the observations. However, the predicted intensity of the plume remains subject to a high uncertainty.

7 Conclusion and perspectives

455 In this paper, we study the input of the assimilation of volcanic SO₂ total columns from TROPOMI, IASI and both TROPOMI and IASI into the CTM MOCAGE in the case of the La Soufrière Saint-Vincent eruption between 9th and 15th April 2021. For the background error covariance matrix, we used a profile containing high values in the volcanic plume vertical range extension. We considered a plume ranging from 9km to 21km, corresponding to 90% of the SO₂ plume heights diagnosed by the TROPOMI Layer Height product.

460

Thanks to the assimilation of TROPOMI and IASI instruments, a SO₂ plume is simulated in MOCAGE. This plume is modelled more or less early and corrected more or less often, depending on the time of the satellite overpass and on the instrument technology. The assimilation of both TROPOMI and IASI instruments leads to a larger plume and a more important amount of SO₂ in the model. During this eruption, MOCAGE is able to simulate the process of converting SO₂ into sulfate aerosols.

465 A sulfate plume, stronger by assimilating only TROPOMI, is computed by MOCAGE. With this creation of sulfate aerosols, AOD increases slightly. Nevertheless, few AOD observations are available during the studied period. Compared with SO₂ total columns observations, the number of pixel stronger than 1 DU in the model is too large but the probability to detect a SO₂ total column is important. In the model, number of points with a total column stronger than 5 DU is close to the number of grid cells with a median observation stronger than 5 DU, especially when IASI and TROPOMI are assimilated. Compared to
470 independent observations from OMI, the probability to detect values stronger than 5 DU is better is better when assimilating observations from both instruments.

Using assimilation outputs to compute forecasts improves the representation of SO₂ total columns in the model. The size and the shape of the plume depends on the forecast range term. The more the forecast range term is small, the more the plume
475 size is important. Sometimes and especially for low values of SO₂ total column, the size of the modelling plume is too large compared to the observations. Concerning the probability to detect a SO₂ total column stronger than a threshold, it is generally better for the short term forecast.

One potential source of discrepancy is the assumptions regarding the altitude and thickness of the plume, which are dynamic
480 in space and time. An inaccurate representation of the SO₂ plume height within the model could lead to a more dispersed plume

or, depending on wind shear conditions, could result in the plume drifting in an incorrect direction. To refine our assimilation process, we could incorporate observed volcanic SO₂ plume heights from both IASI and TROPOMI. This approach, as suggested by (Inness et al., 2021), would likely yield a more accurate simulation of the altitude of the plume, thereby producing a modelled plume shape that better reflects reality.

485

Another factor contributing to the overestimation of the plume extent within the MOCAGE model is the assimilation settings. Specifically, the application of an excessively large horizontal and vertical correlation length could lead to a too extended plume both on the vertical and the horizontal dimensions. Moreover, the chosen standard deviation for the background error can significantly influence the simulated intensity of the plume. With a too large value, the SO₂ plume concentration can be underestimated in MOCAGE whereas with a too small value, the plume intensity can be too strong.

490

Additionally, inherent uncertainties in the model itself must be considered. The chemical processes involving SO₂, including reactions that may not be fully captured, introduce additional complexity into the simulation. Furthermore, the meteorological data driving the model are not without their uncertainties, which can compound the challenges in accurately modelling the transport and transformation of SO₂ emissions.

495

Satellites can give information on the locations where no SO₂ is detected. The use of this information for the assimilation could improve the process because it allows to limit the shape of the plume.

To facilitate the assimilation of the SO₂, particularly the convergence of the minimizer, we could also use a prior volcanic SO₂ emission. In fact, the model and the observations are very different, sometimes by several orders of magnitude. To estimate volcanic SO₂ emissions, a source inversion of the volcanic SO₂ could be used (Boichu et al., 2013).

500

We also have seen that the more frequently the model is corrected, the closer it is to the observations. Assimilating additional instruments would therefore improve assimilation of the SO₂. The best option would be to assimilate observations from geostationary satellites covering the globe.

505

Finally, we made a specific adjustment for this eruption. Ideally, we would like to have a task running daily with assimilation settings that would allow us to assimilate the volcanic SO₂ for each eruption.

Code availability. The code used to generate the analysis (MOCAGE and its variational assimilation suite) is a research-operational code property of Météo France and CERFACS and is not publicly available yet. The readers interested in obtaining parts of the code for research purposes can contact the authors of this study directly.

510



Data availability. All results are available upon request to the authors. Relevant model outputs used to draw the figures will be uploaded to Zenodo shortly.

Author contributions. MB and VG designed this study. MB carried out and interpreted the simulations with JA during his internship supervised by MB and VG. MB is the main contributor to the manuscript. VG and JA reviewed and contributed to the manuscript.

515 *Competing interests.* No competing interest.

Acknowledgements. We want to thank Emanuele Emili for the scientific advice and Pascal Hedelt for providing TROPOMI Layer Height product and give information in the use of this product.



References

- Bennis, K. and Venzke, E.: Report on Soufriere St. Vincent (Saint Vincent and the Grenadines), Bulletin of the Global Volcanism Network, 520 46, <https://doi.org/10.5479/si.GVP.BGVN202105-360150>, 2021.
- Boichu, M., Menut, L., Khvorostyanov, D., Clarisse, L., Clerbaux, C., Turquety, S., and Coheur, P.-F.: Inverting for volcanic SO₂ flux at high temporal resolution using spaceborne plume imagery and chemistry-transport modelling: the 2010 Eyjafjallajökull eruption case study, 13, 8569–8584, <https://doi.org/10.5194/acp-13-8569-2013>, publisher: Copernicus GmbH, 2013.
- Bouysse, F., Berre, L., Bénichou, H., Chambon, P., Girardot, N., Guidard, V., Loo, C., Mahfouf, J.-F., Moll, P., Payan, C., and Raspaud, D.: 525 The 2020 Global Operational NWP Data Assimilation System at Météo-France, 4, 645–664, https://doi.org/10.1007/978-3-030-77722-7_25, 2022.
- Brenot, H., Theys, N., Clarisse, L., van Geffen, J., van Gent, J., Van Roozendaal, M., van der A, R., Hurtmans, D., Coheur, P.-F., Clerbaux, C., Valks, P., Hedelt, P., Prata, F., Rasson, O., Sievers, K., and Zehner, C.: Support to Aviation Control Service (SACS): an online service for near-real-time satellite monitoring of volcanic plumes, 14, 1099–1123, <https://doi.org/10.5194/nhess-14-1099-2014>, publisher: 530 Copernicus GmbH, 2014.
- Brenot, H., Theys, N., Clarisse, L., van Gent, J., Hurtmans, D. R., Vandenbussche, S., Papagiannopoulos, N., Mona, L., Virtanen, T., Uppstu, A., Sofiev, M., Bugliaro, L., Vázquez-Navarro, M., Hedelt, P., Parks, M. M., Barsotti, S., Coltelli, M., Moreland, W., Scollo, S., Salerno, G., Arnold-Arias, D., Hirtl, M., Peltonen, T., Lahtinen, J., Sievers, K., Lipok, F., Rüfenacht, R., Haefele, A., Hervo, M., Wagenaar, S., Som de Cerff, W., de Laat, J., Apituley, A., Stammes, P., Laffineur, Q., Delcloo, A., Lennart, R., Rokitansky, C.-H., Vargas, A., 535 Kerschbaum, M., Resch, C., Zopp, R., Plu, M., Peuch, V.-H., Van Roozendaal, M., and Wotawa, G.: EUNADICS-AV early warning system dedicated to supporting aviation in the case of a crisis from natural airborne hazards and radionuclide clouds, 21, 3367–3405, <https://doi.org/10.5194/nhess-21-3367-2021>, publisher: Copernicus GmbH, 2021.
- Carn, S. A., Krueger, A. J., Krotkov, N. A., Yang, K., and Evans, K.: Tracking volcanic sulfur dioxide clouds for aviation hazard mitigation, 51, 325–343, <https://doi.org/10.1007/s11069-008-9228-4>, 2009.
- 540 Carn, S. A., Clarisse, L., and Prata, A. J.: Multi-decadal satellite measurements of global volcanic degassing, 311, 99–134, <https://doi.org/10.1016/j.jvolgeores.2016.01.002>, 2016.
- Clarisse, L., Hurtmans, D., Clerbaux, C., Hadji-Lazaro, J., Ngadi, Y., and Coheur, P.-F.: Retrieval of sulphur dioxide from the infrared atmospheric sounding interferometer (IASI), 5, 581–594, <https://doi.org/10.5194/amt-5-581-2012>, publisher: Copernicus GmbH, 2012.
- Clarisse, L., Coheur, P.-F., Theys, N., Hurtmans, D., and Clerbaux, C.: The 2011 Nabro eruption, a SO₂ plume height analysis using IASI 545 measurements, 14, 3095–3111, <https://doi.org/10.5194/acp-14-3095-2014>, publisher: Copernicus GmbH, 2014.
- Clerbaux, C., Boynard, A., Clarisse, L., George, M., Hadji-Lazaro, J., Herbin, H., Hurtmans, D., Pommier, M., Razavi, A., Turquety, S., Wespes, C., and Coheur, P.-F.: Monitoring of atmospheric composition using the thermal infrared IASI/MetOp sounder, 9, 6041–6054, <https://doi.org/10.5194/acp-9-6041-2009>, publisher: Copernicus GmbH, 2009.
- Cornut, F., El Amraoui, L., Cuesta, J., Schmitter, R., Blanc, J., and Josse, B.: Assimilation of Aerosol Observations from the Future 550 Spaceborne Lidar Onboard the AOS Mission into the MOCAGE Chemistry: Transport Model, in: Proceedings of the 30th International Laser Radar Conference, edited by Sullivan, J. T., Leblanc, T., Tucker, S., Demoz, B., Eloranta, E., Hostetler, C., Ishii, S., Mona, L., Moshary, F., Papayannis, A., and Rupavatharam, K., pp. 645–651, Springer International Publishing, ISBN 978-3-031-37818-8, https://doi.org/10.1007/978-3-031-37818-8_83, 2023.
- Courtier, P.: The ARPEGE Project at Météo-France, pp. 9–13, 1991.



- 555 Cussac, M., Marécal, V., Thouret, V., Josse, B., and Sauvage, B.: The impact of biomass burning on upper tropospheric carbon monoxide: a study using MOCAGE global model and IAGOS airborne data, 20, 9393–9417, <https://doi.org/10.5194/acp-20-9393-2020>, publisher: Copernicus GmbH, 2020.
- Descheemaeker, M., Plu, M., Marécal, V., Claeyman, M., Olivier, F., Aoun, Y., Blanc, P., Wald, L., Guth, J., Sič, B., Vidot, J., Piacentini, A., and Josse, B.: Monitoring aerosols over Europe: an assessment of the potential benefit of assimilating the VIS04 measurements from the
560 future MTG/FCI geostationary imager, 12, 1251–1275, <https://doi.org/10.5194/amt-12-1251-2019>, publisher: Copernicus GmbH, 2019.
- El Aabaribaoune, M., Emili, E., and Guidard, V.: Estimation of the error covariance matrix for IASI radiances and its impact on the assimilation of ozone in a chemistry transport model, 14, 2841–2856, <https://doi.org/10.5194/amt-14-2841-2021>, publisher: Copernicus GmbH, 2021.
- El Amraoui, L., Plu, M., Guidard, V., Cornut, F., and Bacles, M.: A Pre-Operational System Based on the Assimilation of MODIS Aerosol
565 Optical Depth in the MOCAGE Chemical Transport Model, 14, 1949, <https://doi.org/10.3390/rs14081949>, number: 8 Publisher: Multidisciplinary Digital Publishing Institute, 2022.
- Emili, E., Barret, B., Massart, S., Le Flochmoen, E., Piacentini, A., El Amraoui, L., Pannekoucke, O., and Cariolle, D.: Combined assimilation of IASI and MLS observations to constrain tropospheric and stratospheric ozone in a global chemical transport model, 14, 177–198, <https://doi.org/10.5194/acp-14-177-2014>, publisher: Copernicus GmbH, 2014.
- 570 European Space Agency: TROPOMI Level 2 Sulphur Dioxide, Tech. rep., European Space Agency, <https://doi.org/10.5270/S5P-74eidii>, type: dataset, 2020.
- Feinberg, A., Sukhodolov, T., Luo, B.-P., Rozanov, E., Winkel, L. H. E., Peter, T., and Stenke, A.: Improved tropospheric and stratospheric sulfur cycle in the aerosol–chemistry–climate model SOCOL-AERv2, 12, 3863–3887, <https://doi.org/10.5194/gmd-12-3863-2019>, publisher: Copernicus GmbH, 2019.
- 575 Flemming, J. and Inness, A.: Volcanic sulfur dioxide plume forecasts based on UV satellite retrievals for the 2011 Grímsvötn and the 2010 Eyjafjallajökull eruption, 118, 10,172–10,189, <https://doi.org/10.1002/jgrd.50753>, <https://onlinelibrary.wiley.com/doi/pdf/10.1002/jgrd.50753>, 2013.
- Gouhier, M., Deslandes, M., Guéhenneux, Y., Hereil, P., Cacault, P., and Josse, B.: Operational Response to Volcanic Ash Risks Using HOTVOLC Satellite-Based System and MOCAGE-Accident Model at the Toulouse VAAC, 11, 864,
580 <https://doi.org/10.3390/atmos11080864>, number: 8 Publisher: Multidisciplinary Digital Publishing Institute, 2020.
- Guth, J., Josse, B., Marécal, V., Joly, M., and Hamer, P.: First implementation of secondary inorganic aerosols in the MOCAGE version R2.15.0 chemistry transport model, 9, 137–160, <https://doi.org/10.5194/gmd-9-137-2016>, publisher: Copernicus GmbH, 2016.
- Hedelt, P., Efremenko, D. S., Loyola, D. G., Spurr, R., and Clarisse, L.: Sulfur dioxide layer height retrieval from Sentinel-5 Precursor/TROPOMI using FP_ILM, 12, 5503–5517, <https://doi.org/10.5194/amt-12-5503-2019>, publisher: Copernicus GmbH, 2019.
- 585 Huijnen, V., Williams, J., van Weele, M., van Noije, T., Krol, M., Dentener, F., Segers, A., Houweling, S., Peters, W., de Laat, J., Boersma, F., Bergamaschi, P., van Velthoven, P., Le Sager, P., Eskes, H., Alkemade, F., Scheele, R., Nédélec, P., and Pätz, H.-W.: The global chemistry transport model TM5: description and evaluation of the tropospheric chemistry version 3.0, 3, 445–473, <https://doi.org/10.5194/gmd-3-445-2010>, publisher: Copernicus GmbH, 2010.
- Inness, A., Ades, M., Balis, D., Efremenko, D., Flemming, J., Hedelt, P., Koukouli, M.-E., Loyola, D., and Ribas, R.: The CAMS volcanic forecasting system utilizing near-real time data assimilation of S5P/TROPOMI SO₂ retrievals, Geoscientific Model Development
590 Discussions, 2021, 1–28, 2021.



- Inness, A., Ades, M., Balis, D., Efremenko, D., Flemming, J., Hedelt, P., Koukouli, M.-E., Loyola, D., and Ribas, R.: Evaluating the assimilation of S5P/TROPOMI near real-time SO₂ columns and layer height data into the CAMS integrated forecasting system (CY47R1), based on a case study of the 2019 Raikoke eruption, 15, 971–994, <https://doi.org/10.5194/gmd-15-971-2022>, publisher: Copernicus GmbH, 2022.
- Josse, B., Simon, P., and Peuch, V. H.: Radon global simulations with the multiscale chemistry and transport model MOCAGE, 56, 339–356, <https://doi.org/10.3402/tellusb.v56i4.16448>, publisher: Taylor & Francis _eprint: <https://doi.org/10.3402/tellusb.v56i4.16448>, 2004.
- Kaiser, J. W., Heil, A., Andreae, M. O., Benedetti, A., Chubarova, N., Jones, L., Morcrette, J.-J., Razinger, M., Schultz, M. G., Suttie, M., and van der Werf, G. R.: Biomass burning emissions estimated with a global fire assimilation system based on observed fire radiative power, 9, 527–554, <https://doi.org/10.5194/bg-9-527-2012>, publisher: Copernicus GmbH, 2012.
- Koukouli, M.-E., Michailidis, K., Hedelt, P., Taylor, I. A., Inness, A., Clarisse, L., Balis, D., Efremenko, D., Loyola, D., Grainger, R. G., and Retscher, C.: Volcanic SO₂ layer height by TROPOMI/S5P: evaluation against IASI/MetOp and CALIOP/CALIPSO observations, 22, 5665–5683, <https://doi.org/10.5194/acp-22-5665-2022>, publisher: Copernicus GmbH, 2022.
- Lamarque, J.-F., Bond, T. C., Eyring, V., Granier, C., Heil, A., Klimont, Z., Lee, D., Liousse, C., Mieville, A., Owen, B., Schultz, M. G., Shindell, D., Smith, S. J., Stehfest, E., Van Aardenne, J., Cooper, O. R., Kainuma, M., Mahowald, N., McConnell, J. R., Naik, V., Riahi, K., and van Vuuren, D. P.: Historical (1850–2000) gridded anthropogenic and biomass burning emissions of reactive gases and aerosols: methodology and application, 10, 7017–7039, <https://doi.org/10.5194/acp-10-7017-2010>, publisher: Copernicus GmbH, 2010.
- Lamotte, C., Guth, J., Marécal, V., Cussac, M., Hamer, P. D., Theys, N., and Schneider, P.: Modeling study of the impact of SO₂ volcanic passive emissions on the tropospheric sulfur budget, 21, 11 379–11 404, <https://doi.org/10.5194/acp-21-11379-2021>, publisher: Copernicus GmbH, 2021.
- Lechner, P., Tupper, A., Guffanti, M., Loughlin, S., and Casadevall, T.: Volcanic Ash and Aviation—The Challenges of Real-Time, Global Communication of a Natural Hazard, in: *Observing the Volcano World: Volcano Crisis Communication*, edited by Fearnley, C. J., Bird, D. K., Haynes, K., McGuire, W. J., and Jolly, G., pp. 51–64, Springer International Publishing, ISBN 978-3-319-44097-2, https://doi.org/10.1007/11157_2016_49, 2018.
- Lefevre, F., Brasseur, G., Folkins, I., Smith, A., and Simon, P.: Chemistry of the 1991–1992 stratospheric winter: Three-dimensional model simulations, 99, 8183–8195, <https://doi.org/10.1029/93JD03476>, _eprint: <https://onlinelibrary.wiley.com/doi/pdf/10.1029/93JD03476>, 1994.
- Li, C., Krotkov, N. A., Carn, S., Zhang, Y., Spurr, R. J. D., and Joiner, J.: New-generation NASA Aura Ozone Monitoring Instrument (OMI) volcanic SO₂ dataset: algorithm description, initial results, and continuation with the Suomi-NPP Ozone Mapping and Profiler Suite (OMPS), 10, 445–458, <https://doi.org/10.5194/amt-10-445-2017>, publisher: Copernicus GmbH, 2017.
- Marécal, V., Peuch, V.-H., Andersson, C., Andersson, S., Arteta, J., Beekmann, M., Benedictow, A., Bergström, R., Bessagnet, B., Cansado, A., Chéroux, F., Colette, A., Coman, A., Curier, R. L., Denier van der Gon, H. a. C., Drouin, A., Elbern, H., Emili, E., Engelen, R. J., Eskes, H. J., Foret, G., Friese, E., Gauss, M., Giannaros, C., Guth, J., Joly, M., Jaumouillé, E., Josse, B., Kadyrov, N., Kaiser, J. W., Krajsek, K., Kuenen, J., Kumar, U., Liora, N., Lopez, E., Malherbe, L., Martinez, I., Melas, D., Meleux, F., Menut, L., Moinat, P., Morales, T., Parmentier, J., Piacentini, A., Plu, M., Poupkou, A., Queguiner, S., Robertson, L., Rouïl, L., Schaap, M., Segers, A., Sofiev, M., Tarasson, L., Thomas, M., Timmermans, R., Valdebenito, , van Velthoven, P., van Versendaal, R., Vira, J., and Ung, A.: A regional air quality forecasting system over Europe: the MACC-II daily ensemble production, 8, 2777–2813, <https://doi.org/10.5194/gmd-8-2777-2015>, publisher: Copernicus GmbH, 2015.



- Prata, A. J.: Satellite detection of hazardous volcanic clouds and the risk to global air traffic, 51, 303–324, <https://doi.org/10.1007/s11069-008-9273-z>, 2009.
- Prata, F., Woodhouse, M., Huppert, H. E., Prata, A., Thordarson, T., and Carn, S.: Atmospheric processes affecting the separation of volcanic ash and SO₂ in volcanic eruptions: inferences from the May 2011 Grímsvötn eruption, 17, 10709–10732, <https://doi.org/10.5194/acp-17-10709-2017>, publisher: Copernicus GmbH, 2017.
- Price, C., Penner, J., and Prather, M.: NO_x from lightning: 1. Global distribution based on lightning physics, 102, 5929–5941, <https://doi.org/10.1029/96JD03504>, _eprint: <https://onlinelibrary.wiley.com/doi/pdf/10.1029/96JD03504>, 1997.
- Qu, Z., Henze, D. K., Li, C., Theys, N., Wang, Y., Wang, J., Wang, W., Han, J., Shim, C., Dickerson, R. R., and Ren, X.: SO₂ Emission Estimates Using OMI SO₂ Retrievals for 2005–2017, 124, 8336–8359, <https://doi.org/10.1029/2019JD030243>, _eprint: <https://onlinelibrary.wiley.com/doi/pdf/10.1029/2019JD030243>, 2019.
- Rodgers, C. D. and Connor, B. J.: Intercomparison of remote sounding instruments, 108, <https://doi.org/10.1029/2002JD002299>, _eprint: <https://onlinelibrary.wiley.com/doi/pdf/10.1029/2002JD002299>, 2003.
- Rouil, L., Honoré, C., Vautard, R., Beekmann, M., Bessagnet, B., Malherbe, L., Meleux, F., Dufour, A., Elichegaray, C., Flaud, J.-M., Menut, L., Martin, D., Peuch, A., Peuch, V.-H., and Poisson, N.: Prev'air: An Operational Forecasting and Mapping System for Air Quality in Europe, 90, 73–84, <https://doi.org/10.1175/2008BAMS2390.1>, publisher: American Meteorological Society Section: Bulletin of the American Meteorological Society, 2009.
- Schmidt, A., Witham, C. S., Theys, N., Richards, N. A. D., Thordarson, T., Szpek, K., Feng, W., Hort, M. C., Woolley, A. M., Jones, A. R., Redington, A. L., Johnson, B. T., Hayward, C. L., and Carslaw, K. S.: Assessing hazards to aviation from sulfur dioxide emitted by explosive Icelandic eruptions, 119, 14,180–14,196, <https://doi.org/10.1002/2014JD022070>, _eprint: <https://onlinelibrary.wiley.com/doi/pdf/10.1002/2014JD022070>, 2014.
- Sears, T. M., Thomas, G. E., Carboni, E., A. Smith, A. J., and Grainger, R. G.: SO₂ as a possible proxy for volcanic ash in aviation hazard avoidance, 118, 5698–5709, <https://doi.org/10.1002/jgrd.50505>, _eprint: <https://onlinelibrary.wiley.com/doi/pdf/10.1002/jgrd.50505>, 2013.
- Sellitto, P., Podglajen, A., Belhadji, R., Boichu, M., Carboni, E., Cuesta, J., Duchamp, C., Kloss, C., Siddans, R., Bègue, N., Blarel, L., Jegou, F., Khaykin, S., Renard, J.-B., and Legras, B.: The unexpected radiative impact of the Hunga Tonga eruption of 15th January 2022, 3, 1–10, <https://doi.org/10.1038/s43247-022-00618-z>, publisher: Nature Publishing Group, 2022.
- Sindelarova, K., Granier, C., Bouarar, I., Guenther, A., Tilmes, S., Stavrakou, T., Müller, J.-F., Kuhn, U., Stefani, P., and Knorr, W.: Global data set of biogenic VOC emissions calculated by the MEGAN model over the last 30 years, 14, 9317–9341, <https://doi.org/10.5194/acp-14-9317-2014>, publisher: Copernicus GmbH, 2014.
- Sič, B., El Amraoui, L., Marécal, V., Josse, B., Arteta, J., Guth, J., Joly, M., and Hamer, P. D.: Modelling of primary aerosols in the chemical transport model MOCAGE: development and evaluation of aerosol physical parameterizations, 8, 381–408, <https://doi.org/10.5194/gmd-8-381-2015>, publisher: Copernicus GmbH, 2015.
- Sič, B., El Amraoui, L., Piacentini, A., Marécal, V., Emili, E., Cariolle, D., Prather, M., and Attié, J.-L.: Aerosol data assimilation in the chemical transport model MOCAGE during the TRAQA/ChArMEX campaign: aerosol optical depth, 9, 5535–5554, <https://doi.org/10.5194/amt-9-5535-2016>, publisher: Copernicus GmbH, 2016.
- Spurr, R., de Haan, J., van Oss, R., and Vasilkov, A.: Discrete-ordinate radiative transfer in a stratified medium with first-order rotational Raman scattering, 109, 404–425, <https://doi.org/10.1016/j.jqsrt.2007.08.011>, 2008.



- Stockwell, W. R., Kirchner, F., Kuhn, M., and Seefeld, S.: A new mechanism for regional atmospheric chemistry modeling, 102, 25 847–25 879, <https://doi.org/10.1029/97JD00849>, eprint: <https://onlinelibrary.wiley.com/doi/pdf/10.1029/97JD00849>, 1997.
- Theys, N.: S5P/TROPOMI SO₂ ATBD, Tech. rep., Tech. Rep. 1.1. 0, BIRA, available at: <https://sentinels.copernicus.eu> . . . , 2018.
- Theys, N., De Smedt, I., Yu, H., Danckaert, T., van Gent, J., Hörmann, C., Wagner, T., Hedelt, P., Bauer, H., Romahn, F., Pedernana, M., Loyola, D., and Van Roozendael, M.: Sulfur dioxide retrievals from TROPOMI onboard Sentinel-5 Precursor: algorithm theoretical basis, 10, 119–153, <https://doi.org/10.5194/amt-10-119-2017>, publisher: Copernicus GmbH, 2017.
- 670 Theys, N., Hedelt, P., De Smedt, I., Lerot, C., Yu, H., Vlietinck, J., Pedernana, M., Arellano, S., Galle, B., Fernandez, D., Carlito, C. J. M., Barrington, C., Taisne, B., Delgado-Granados, H., Loyola, D., and Van Roozendael, M.: Global monitoring of volcanic SO₂ degassing with unprecedented resolution from TROPOMI onboard Sentinel-5 Precursor, 9, 2643, <https://doi.org/10.1038/s41598-019-39279-y>, publisher: Nature Publishing Group, 2019.
- 675 Thomas, H. E. and Prata, A. J.: Sulphur dioxide as a volcanic ash proxy during the April–May 2010 eruption of Eyjafjallajökull Volcano, Iceland, 11, 6871–6880, <https://doi.org/10.5194/acp-11-6871-2011>, publisher: Copernicus GmbH, 2011.
- Veefkind, J. P., Aben, I., McMullan, K., Förster, H., de Vries, J., Otter, G., Claas, J., Eskes, H. J., de Haan, J. F., Kleipool, Q., van Weele, M., Hasekamp, O., Hoogeveen, R., Landgraf, J., Snel, R., Tol, P., Ingmann, P., Voors, R., Kruizinga, B., Vink, R., Visser, H., and Levelt, P. F.: TROPOMI on the ESA Sentinel-5 Precursor: A GMES mission for global observations of the atmospheric composition for climate, air quality and ozone layer applications, 120, 70–83, <https://doi.org/10.1016/j.rse.2011.09.027>, 2012.
- 680 Vittorioso, F., Guidard, V., and Fourrié, N.: Assessment of the contribution of the Meteosat Third Generation Infrared Sounder (MTG-IRS) for the characterisation of ozone over Europe, 17, 5279–5299, <https://doi.org/10.5194/amt-17-5279-2024>, publisher: Copernicus GmbH, 2024.
- 685 Witze, A.: Why the Tongan eruption will go down in the history of volcanology, 602, 376–378, <https://doi.org/10.1038/d41586-022-00394-y>, bandiera_abtest: a Cg_type: News Feature Publisher: Nature Publishing Group Subject_term: Volcanology, Seismology, Atmospheric science, Geology, 2022.

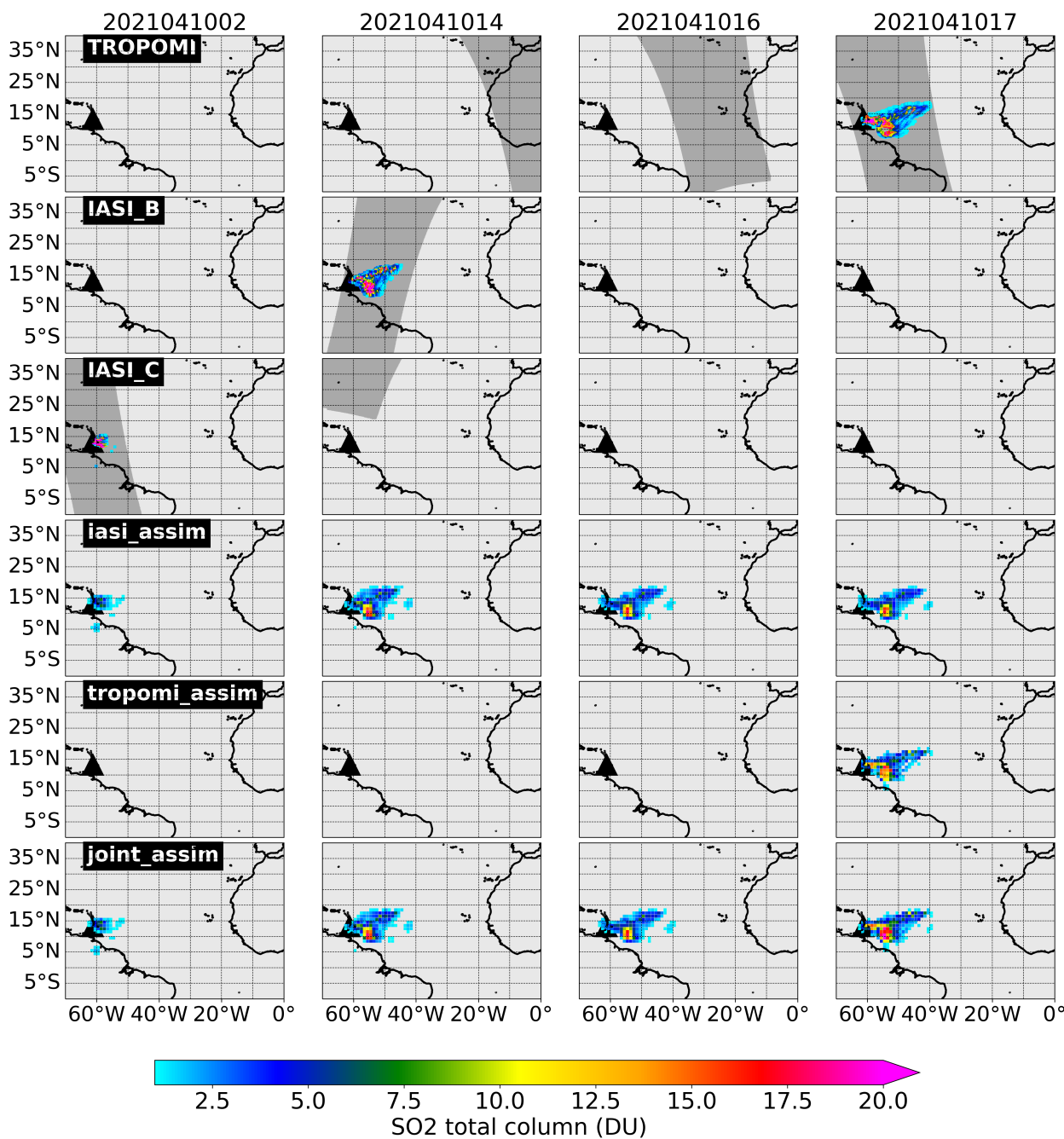


Figure 1. Observations assimilated and analyses of SO₂ total columns on 10th April 2021 at 2, 14, 16 and 17 UTC. The first three rows correspond respectively to TROPOMI, IASI B and IASI C observations. Analysis outputs are plotted on the fourth line for iasi_assim experiment, on the fifth line for tropomi_assim experiment and on the sixth line for the joint_assim experiment. The shaded areas shown on the first 3 lines correspond to areas where there are no observations or where observations have not been assimilated. Observations are not assimilated when they are less than 0.5 DU for IASI and TROPOMI's slant columns are less than 1 DU.

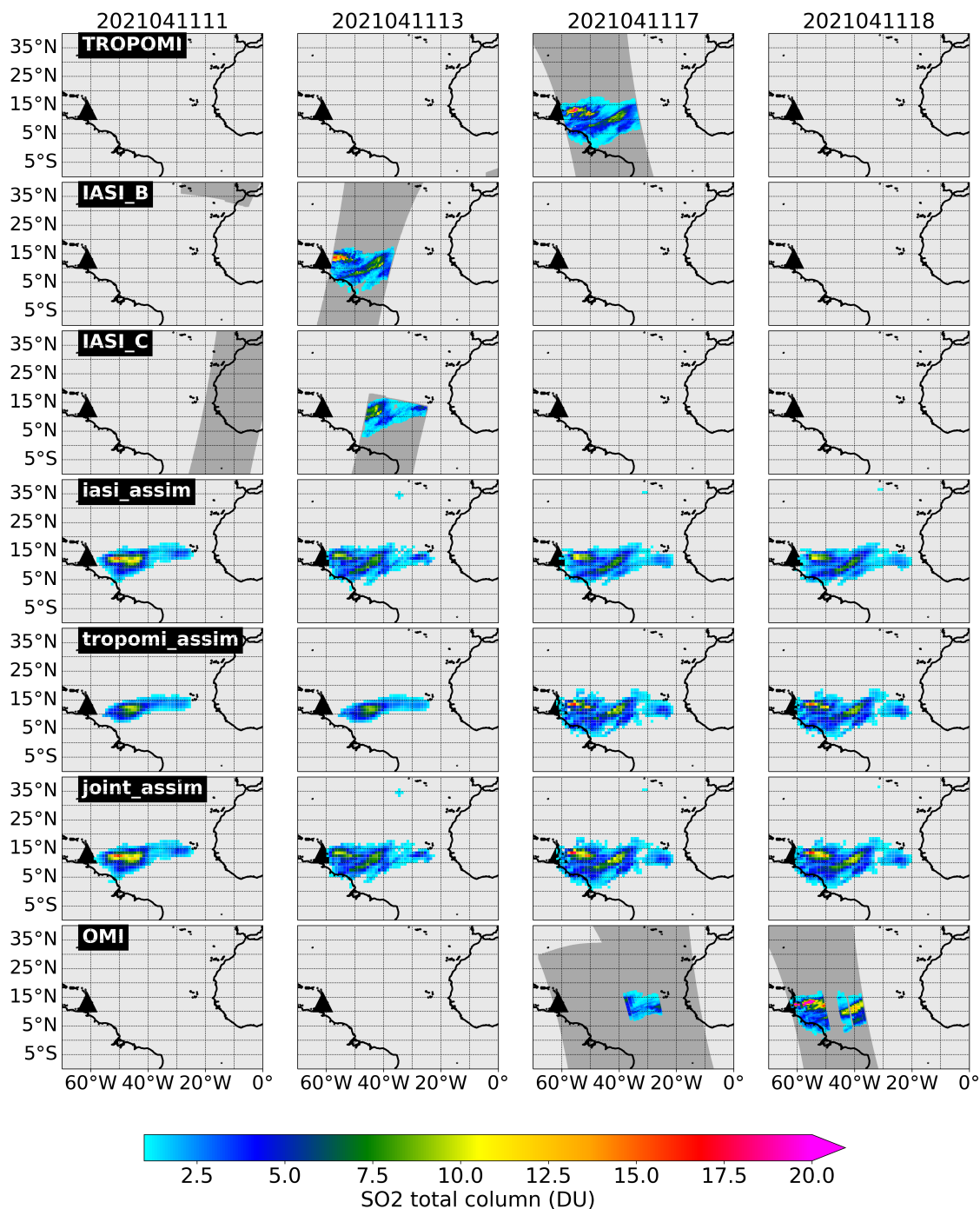


Figure 2. Observations and analyses of SO₂ total columns on 11th April 2021 at 11, 13, 17 and 18 UTC. The first three rows correspond respectively to TROPOMI, IASI B and IASI C observations. The last row corresponds to OMI observations. Analysis outputs are plotted on the fourth line for iasi_assim experiment, on the fifth line for tropomi_assim experiment and on the sixth line for the joint_assim experiment.

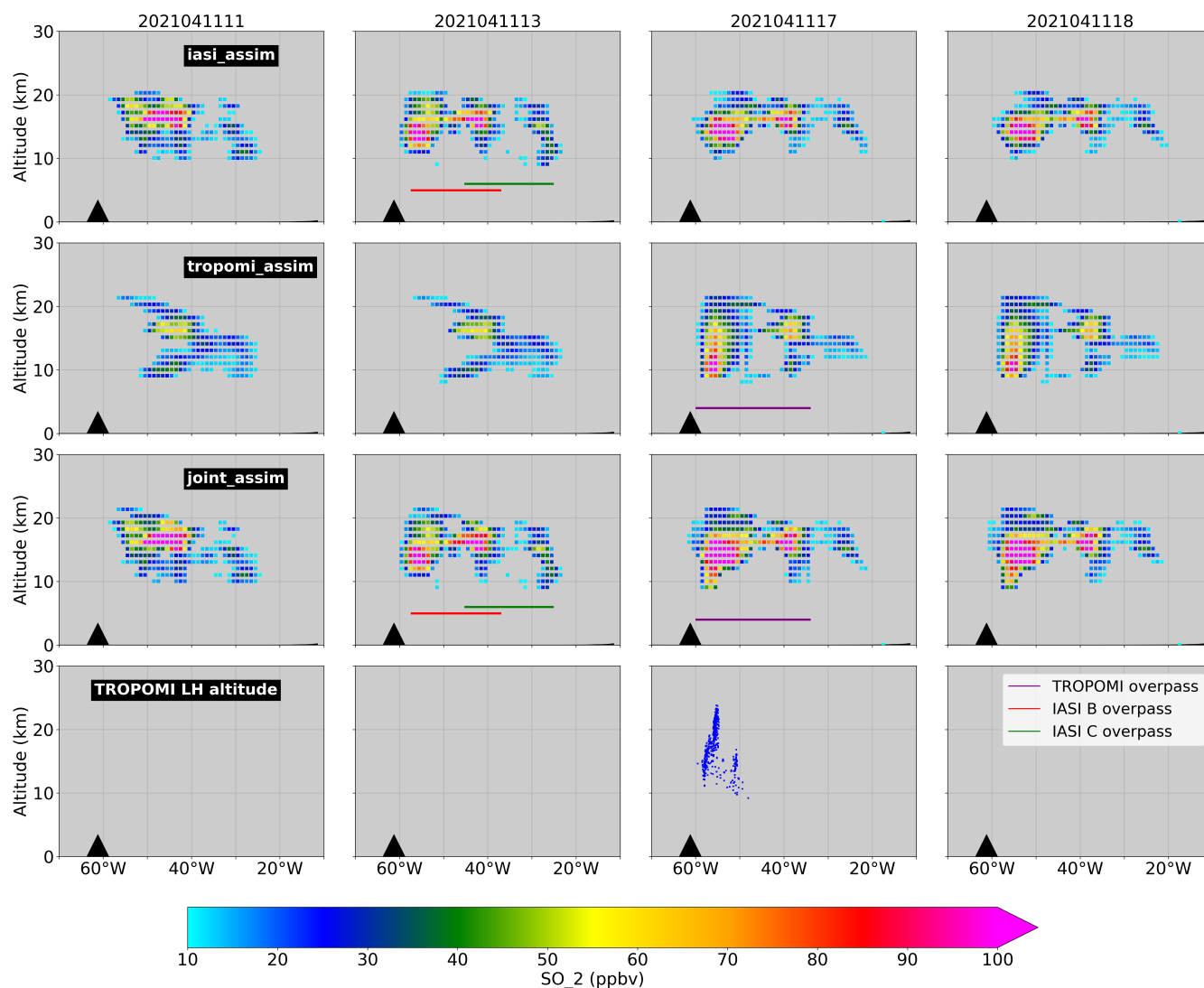


Figure 3. Vertical sections of analysed SO₂ concentration at 13.5°N latitude on 11th April 2021 at 11, 13, 17 and 18 UTC. Rows correspond respectively to the TROPOMI data assimilation, IASI assimilation, joint assimilation and the height of SO₂ plume provided by the TROPOMI Layer Height product.

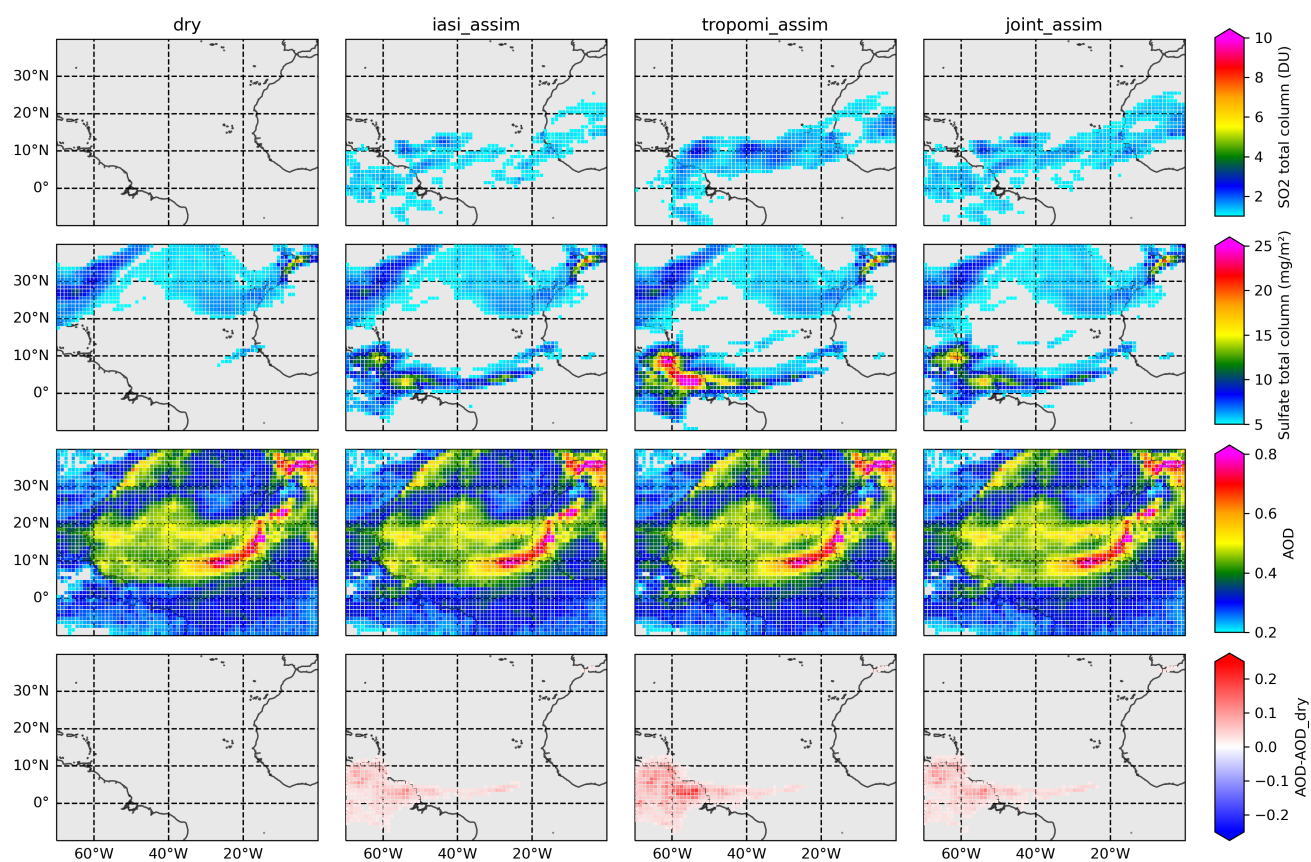


Figure 4. SO₂ total column, sulfate total column, AOD and difference between AOD and AOD of dry experiment on 14th April 2021 at 7 UTC for dry, iasi_assim, tropomi_assim and joint_assim experiments.

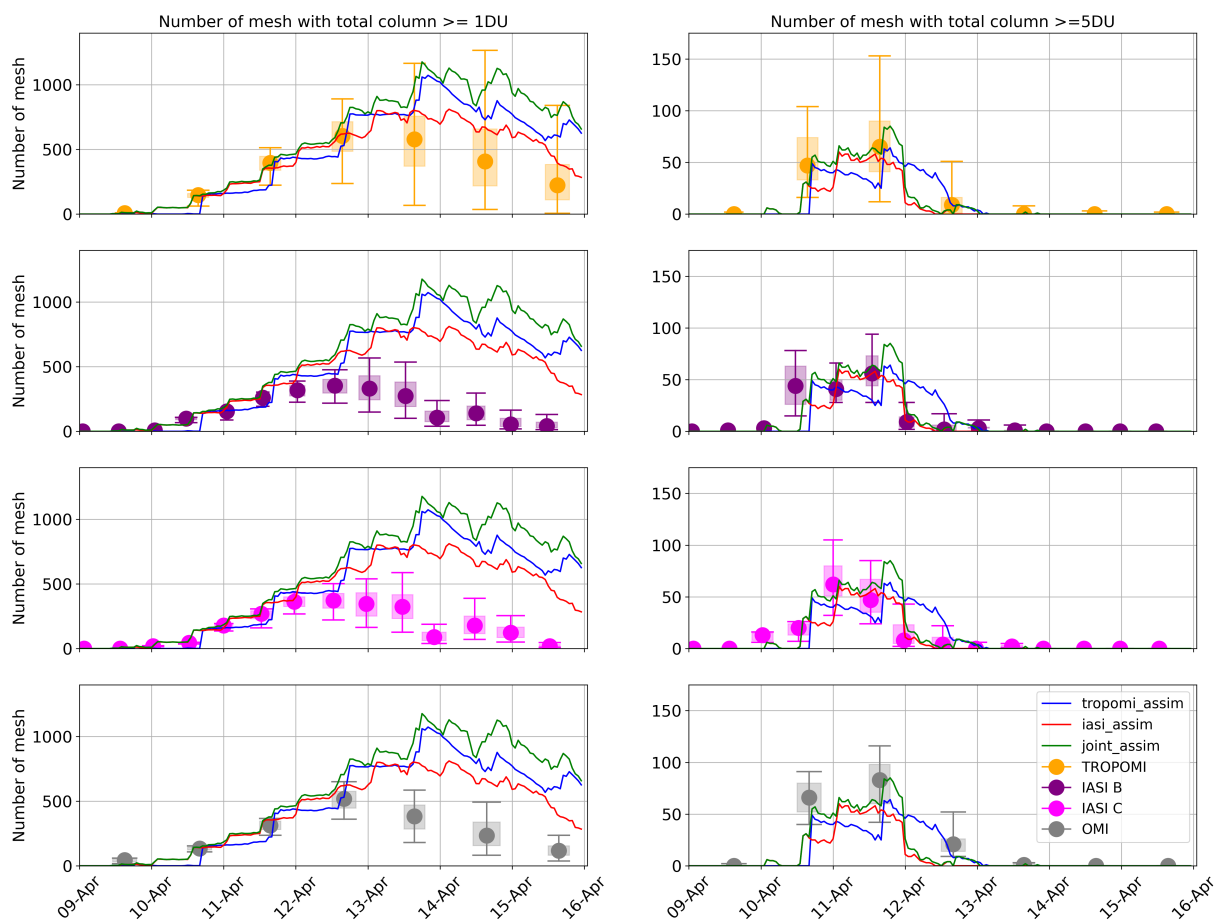


Figure 5. Number of grid cells where analyses exceed 1DU and 5DU. The blue, red and green lines show the number of points at which the total columns reach these thresholds in the tropomi_assim, the iasi_assim and the joint_assim experiments. Orange, purple, magenta and grey boxplots represent the number of grid cells where TROPOMI, IASI B, IASI C and OMI observations exceed the threshold.

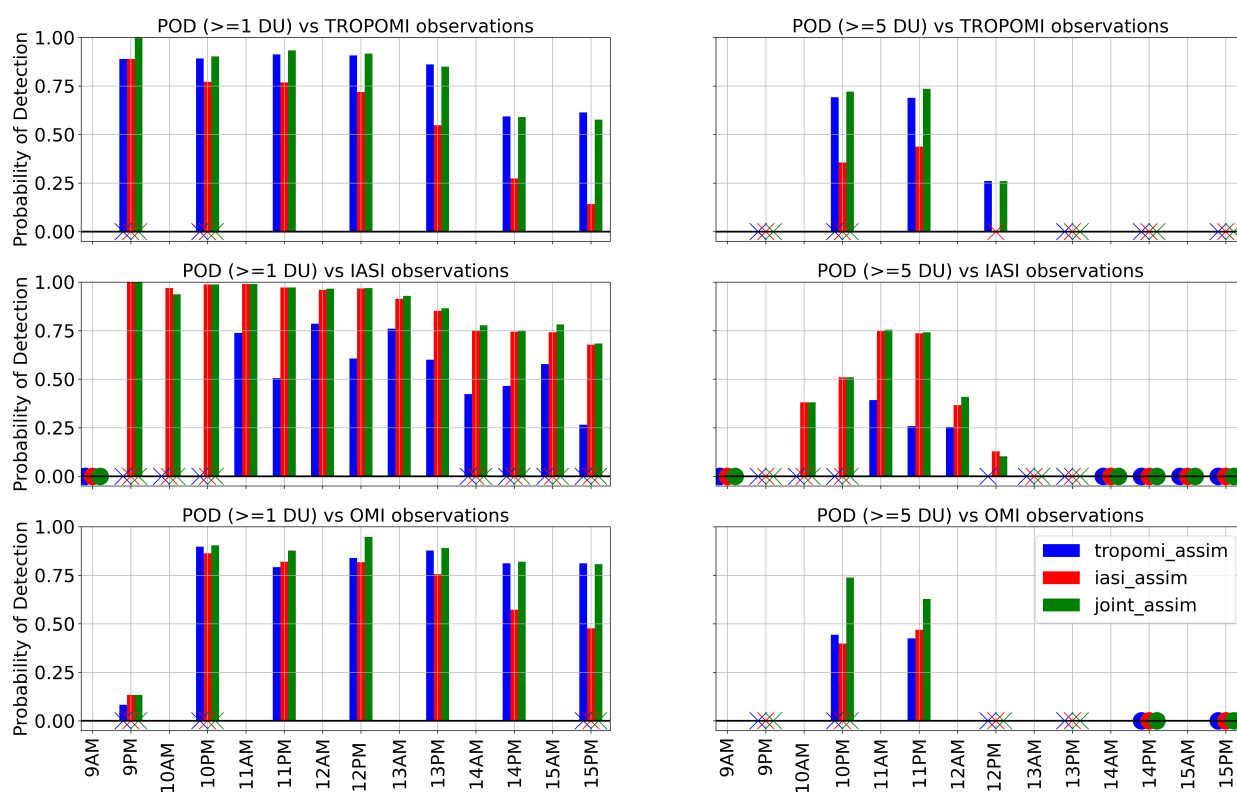


Figure 6. Probability of detection for 1 and 5 DU thresholds for the three experiments: tropomi_assim in blue and iasi_assim in red and joint_assim in green. Dots represent times when there is no observation. Crosses represent the moments when there are only misses events.

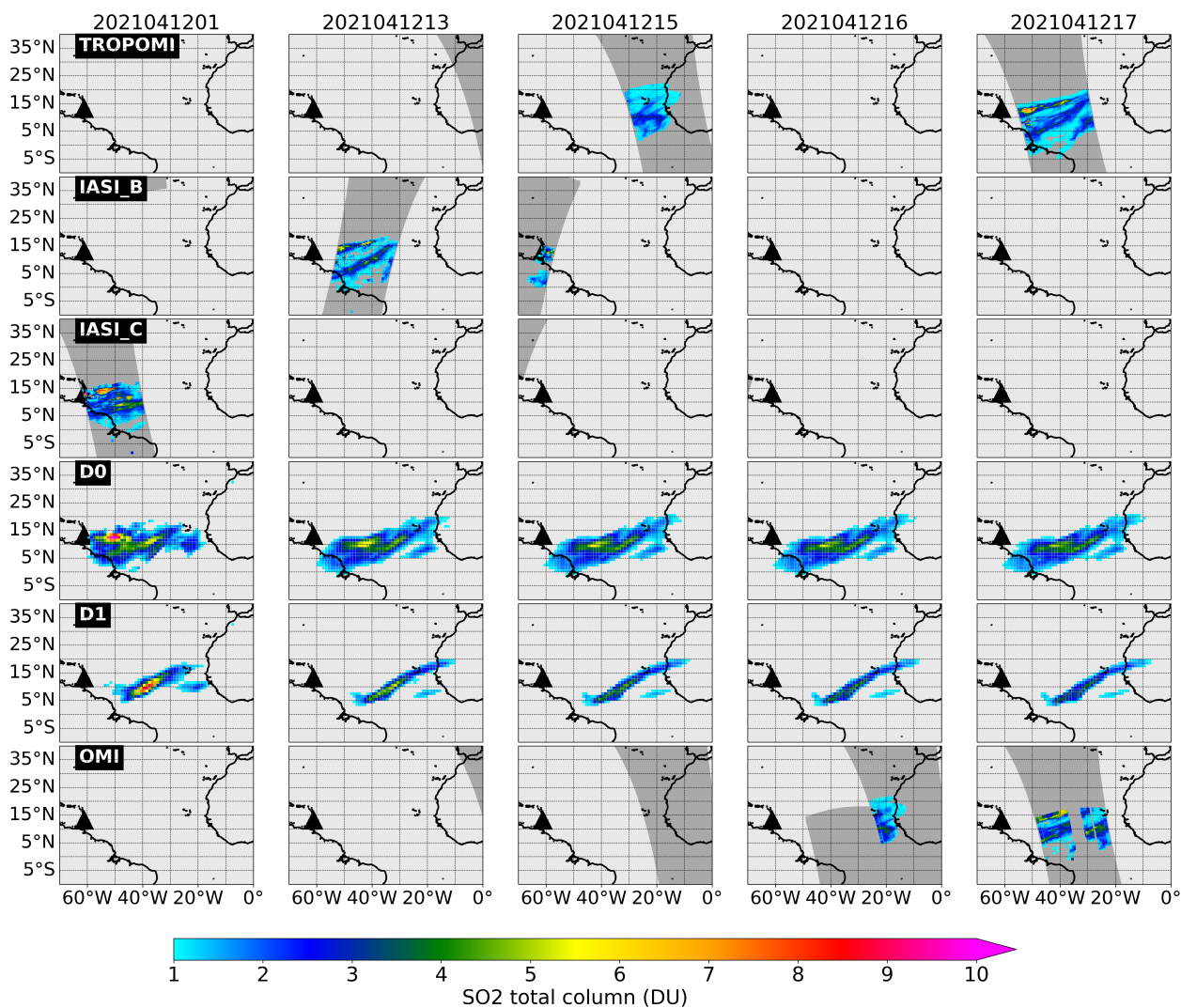


Figure 7. Observations and forecasts of SO₂ total columns on 12th April 2021 at 01, 13, 15, 16, 17 UTC. The first row and the last row correspond to TROPOMI and OMI observations. Forecasts are computed from the 11th April analysis outputs (2nd row) and from the 10th April analysis outputs (3rd row). These forecasts are available on 12th April

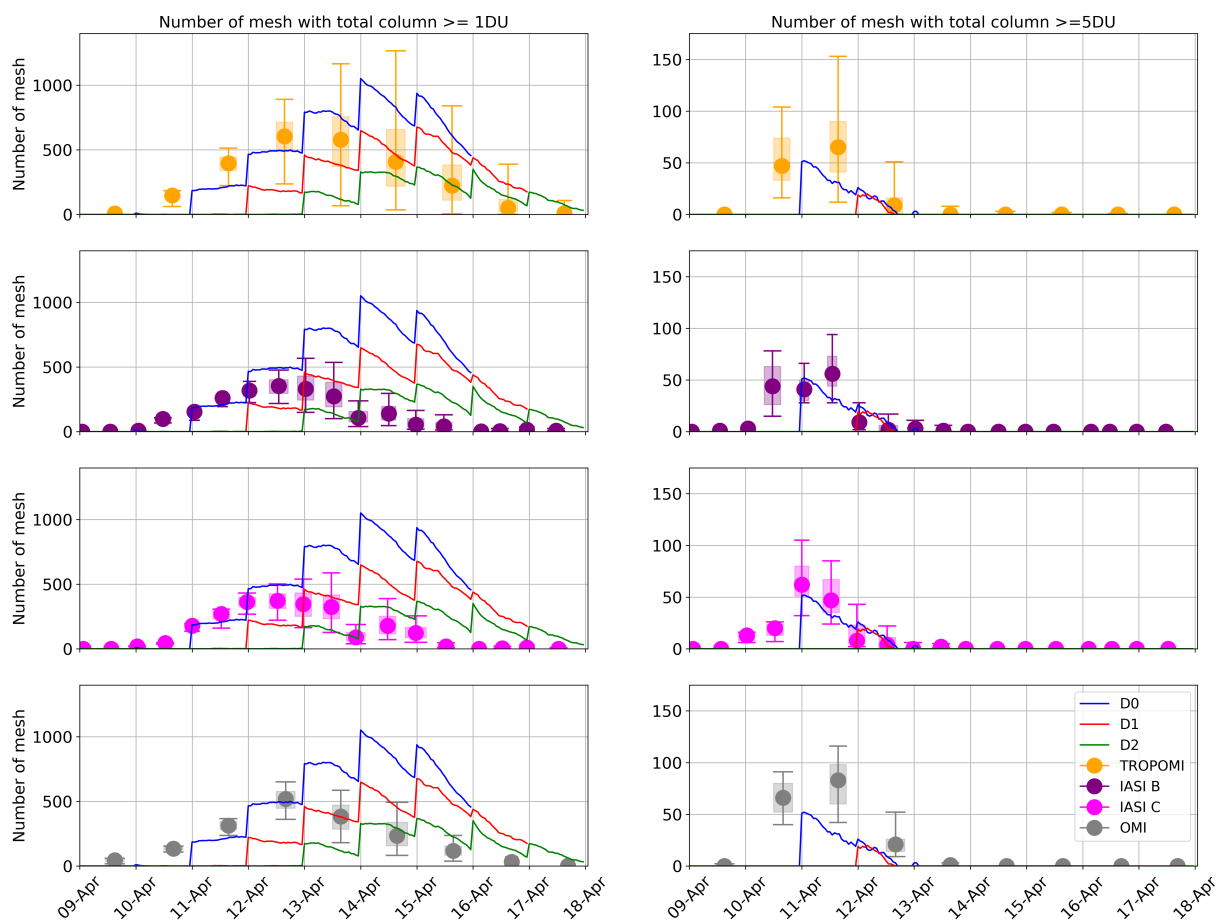


Figure 8. Number of grid cells where forecasts initialised by the joint_assim outputs reaches 1 DU and 5 DU. The blue, red and green lines show the number of points at which the total columns reach these thresholds in the D0, D1 and D2 forecasts. Orange, purple, magenta and grey boxplots represent the number of grid cells where TROPOMI, IASI B, IASI C and OMI observations exceed the threshold.

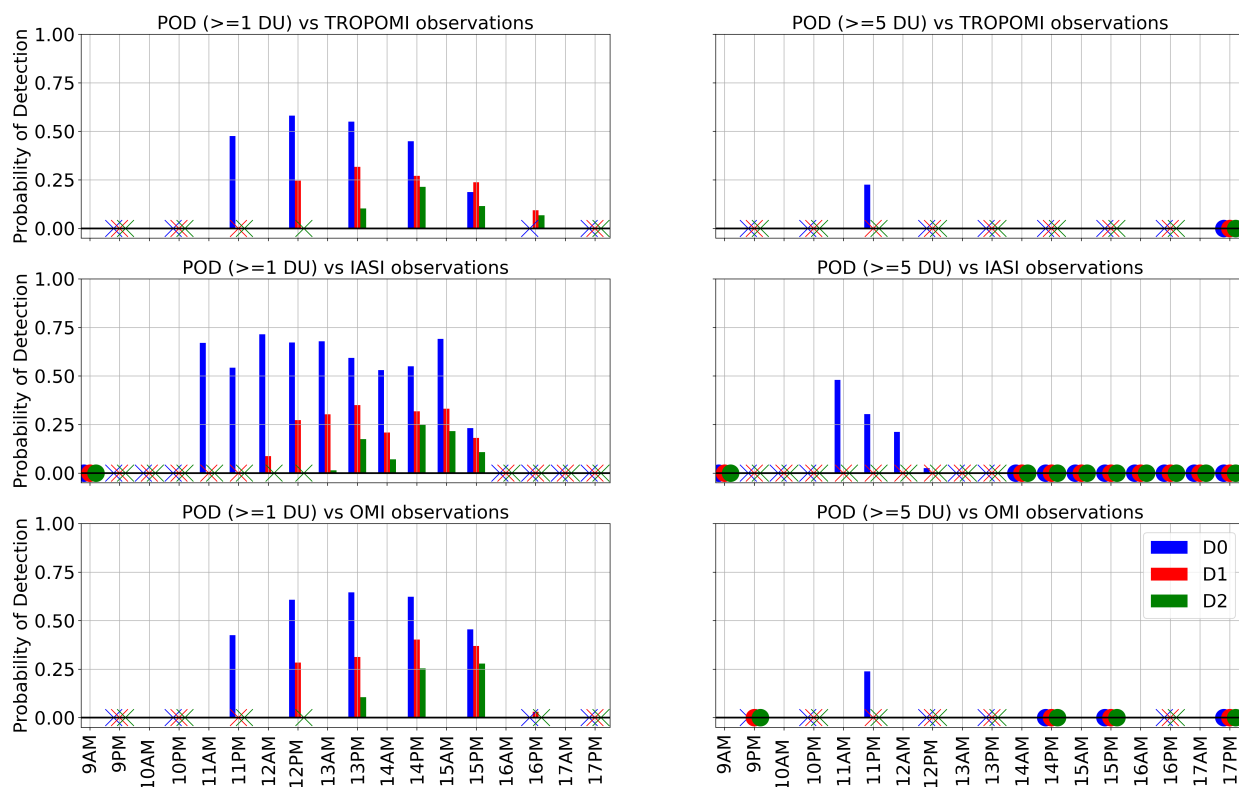


Figure 9. Probability of detection for 1 DU and 5 DU thresholds for the D0 forecast in blue, the D1 forecast in red and the D2 forecast in green. Dots represent times when there is no observation. Crosses represent the moments when there are only misses events.